Functional Magnetic Resonance Imaging Signatures of Pavlovian and Instrumental Valuation Systems during a Modified Orthogonalized Go/No-go Task

Filippo Queirazza[1], J. Douglas Steele[2], Rajeev Krishnadas[1] Jonathan Cavanagh[1], and Marios G. Philiastides[1]

Downloaded from http://direct.mit.edu/jocn/article-pdf/35/12/2089/2170792/jocn_a_02062.pdf by University of Glasgow user on 05 June 2026

Abstract

■ Motivational (i.e., Pavlovian) values interfere with instrumental responding and can lead to suboptimal decision-making. In humans, task-based neuroimaging studies have only recently started illuminating the functional neuroanatomy of Pavlovian biasing of instrumental control. To provide a mechanistic understanding of the neural dynamics underlying the Pavlovian and instrumental valuation systems, analysis of neuroimaging data has been informed by computational modeling of conditioned behavior. Nonetheless, because of collinearities in Pavlovian and instrumental predictions, previous research failed to tease out hemodynamic activity that is parametrically and dynamically modulated by coexistent Pavlovian and instrumental value expectations. Moreover, neural correlates of Pavlovian to instrumental transfer effects have so far only been identified in extinction (i.e., in the absence of learning). In this study, we devised a modified version of the orthogonalized go/no-go paradigm, which introduced Pavlovian-only catch trials to better disambiguate trial-by-trial Pavlovian and instrumental predictions in both sexes. We found that hemodynamic activity in the ventromedial pFC covaried uniquely with the model-derived Pavlovian value expectations. Notably, modulation of neural activity encoding for instrumental predictions in the supplementary motor cortex was linked to successful action selection in conflict conditions. Furthermore, hemodynamic activity in regions pertaining to the limbic system and medial pFC was correlated with synergistic Pavlovian and instrumental predictions and improved conditioned behavior during congruent trials. Altogether, our results provide new insights into the functional neuroanatomy of decision-making and corroborate the validity of our variant of the orthogonalized go/no-go task as a behavioral assay of the Pavlovian and instrumental valuation systems. ■

INTRODUCTION

According to the two-process theory of associative learning, the interaction between the Pavlovian and instrumental valuation systems underpins adaptive behavior (Mackintosh, 1983; Rescorla & Solomon, 1967). Correspondingly, the Pavlovian corrupting influence on optimal instrumental control is thought to underlie well-known behavioral anomalies observed in animals (i.e., autoshaping [Brown & Jenkins, 1968], negative automaintenance [Williams & Williams, 1969]) and humans (i.e., framing [De Martino, Kumaran, Seymour, & Dolan, 2006] and endowment [Kahneman, Knetsch, & Thaler, 1990] effect). Furthermore, there is growing empirical evidence that Pavlovian learning biases may account for maladaptive behaviors associated with depression (Huys et al., 2016; Dayan & Huys, 2008), addiction (Robinson & Berridge, 2003), trauma (Ousdal et al., 2018), and other common mental disorders (Garbusow et al., 2022).

Whereas the Pavlovian system supports the acquisition of associations between temporally contiguous stimuli and outcomes, the instrumental system enables adaptive learning of stimulus–response–outcome pairings. Crucially, because hard-wired, Pavlovian-mediated preparatory responses (i.e., approach vs. avoidance) are tightly tied to outcome valence (i.e., reward vs. punishment), the Pavlovian system invariably prescribes approach to reward-predicting stimuli and avoidance of punishment-predicting stimuli. Conversely, the instrumental system flexibly selects actions based on their contingent outcomes and independently of outcome valence. Therefore, when the required action is not congruent with the anticipated outcome valence (i.e., approach punishment-predicting stimuli or avoid reward-predicting stimuli), Pavlovian and instrumental predictions diverge and compete for behavioral control. Alternatively, when the required action and anticipated outcome valence are congruent (i.e., approach reward-predicting stimuli or avoid punishment-predicting stimuli), Pavlovian and instrumental predictions converge and exert synergistic effects on behavior.

The two most popular experimental paradigms that leverage the asymmetries of Pavlovian and instrumental predictions as a function of the two axes of behavioral control (i.e., valence and action) are the Pavlovian-to-instrumental

[1]University of Glasgow, United Kingdom, [2]University of Dundee, United Kingdom

© 2023 Massachusetts Institute of Technology

Journal of Cognitive Neuroscience 35:12, pp. 2089–2109
https://doi.org/10.1162/jocn_a_02062

transfer (PIT; Cartoni, Puglisi-Allegra, & Baldassarre, 2013) and orthogonalized go/no-go task (Crockett, Clark, & Robbins, 2009). In the PIT task, Pavlovian and instrumental predictions coupled with different cues are acquired in separate experimental stages, and transfer effects are subsequently tested in extinction (i.e., in the absence of new learning). In the orthogonalized go/no-go task, Pavlovian and instrumental predictions coupled with the same cues are continuously updated via probabilistic feedback.

To illuminate the functional neuroanatomy of the Pavlovian–instrumental dichotomy, human studies have exploited hemodynamic responses to Pavlovian and instrumental predictions during acquisition of functional magnetic resonance imaging (fMRI) data (Guitart-Masip, Huys et al., 2012). Moreover, analysis of fMRI recordings has capitalized on the mechanistic insights afforded by the use of reinforcement learning (RL) theory to account for experimentally elicited motor responses (Guitart-Masip, Huys et al., 2012). In the most successful implementations of this modeling work, the linear superposition of Pavlovian and instrumental values into a common decision variable guides action selection (Guitart-Masip, Huys et al., 2012; Huys et al., 2011). Computational models of the PIT effect are usually built on the offline linear combination of static (learned) instrumental and (fitted) Pavlovian value expectations, and thus, parametric modulation of hemodynamic responses as a function of PIT effects is based on behavioral measures such as the strength of instrumental responding (Geurts, Huys, den Ouden, & Cools, 2013). Although RL models of the orthogonalized go/no-go task incorporate online updating of Pavlovian and instrumental values by means of separate prediction errors, the time courses tracking their temporal evolution are highly collinear, thus precluding fMRI modeling of the neural correlates of Pavlovian learning biases (Guitart-Masip, Huys et al., 2012).

In this study, we have addressed this shortcoming and developed a modified version of the orthogonalized go/no-go task to effectively tease apart Pavlovian and instrumental value representations and their interaction in the brain. We included catch trials whereby only Pavlovian expectations were being updated and no instrumental responding was required. We demonstrated parametric encoding of instrumental and Pavlovian predictions in the supplementary motor cortex (SMC) and ventromedial pFC (vmPFC), respectively, and of synergistic Pavlovian–instrumental interaction (PII) effects in regions pertaining to the limbic system. Crucially, we revealed brain-behavior correlations further validating the role of these regions in modulating learning and choice behavior.

METHODS

Participants

We recruited 45 participants for our study. Five participants were excluded because of significant incidental clinical brain imaging finding ($n = 1$), poor task performance (i.e., choice accuracy < 55%; $n = 3$), or technical problems with data acquisition ($n = 1$). The remaining 40 participants (32 women) were included in the analyses presented in this article. Participants were aged between 18 and 60 years (mean = 22.07 years, $SD = \pm 2.32$ years). All participants provided written, informed consent. On the basis of a previously documented large behavioral effect size (Cohen's $d = 1.4$; Guitart-Masip, Huys et al., 2012), we estimated a sample size of 40 participants would be sufficient to achieve 80% power at an alpha level of .05. The study protocol was approved by the University of Glasgow College of Science and Engineering ethics committee (300160098).

Experimental Procedures

To better tease apart the dynamic (i.e., trial-by-trial) neural representations of instrumental and Pavlovian systems in the presence of learning, we modified the popular orthogonalized go/no-go task (Guitart-Masip, Huys et al., 2012). Indeed, the classic version of this task does not allow a straightforward dissociation of Pavlovian and instrumental predictions, and previous work highlighted this shortcoming (Guitart-Masip, Huys et al., 2012). Likewise, classic PIT paradigms are designed to elicit Pavlovian effects on instrumental responding in the absence of new learning and thus are not suited to investigate the "dynamic" effects of the Pavlovian and instrumental systems on decision-making (Huys et al., 2011).

Our task consisted of four blocks. Each block had 40 mixed trials (i.e., instrumental and Pavlovian) and 20 Pavlovian-only trials (60 trials per block and 240 trials in total; Figure 1A and B). Within each block, mixed trials were randomly interspersed with Pavlovian-only trials. In the mixed trials, there were three events: presentation of a fractal cue, target detection, and probabilistic outcome. There were four fractal cues, and each denoted a specific combination between action requirement (i.e., go vs. no-go) and outcome valence (i.e., win vs. lose). The association between the four fractals and the resulting combinations of action and valence (i.e., go to win/no-go to win/go to avoid losing/no-go to avoid losing) were randomized across participants. In the target detection phase, a circle was shown on either the right- or left-hand side of the screen (target positions were counterbalanced across trials within each block). In the outcome phase, possible outcomes were an upward-pointing green arrow (1 point) or a horizontal yellow bar (0 point) in the win trials and a downward-pointing red arrow (−1 point) or a horizontal yellow bar (0 point) in the lose trials. Response–outcome contingencies were probabilistic, as shown in Figure 1B. Correct responses were rewarded with the best possible outcome (i.e., green arrow for the win cues and yellow bar for the lose cues) 80% of the time. Reverse outcome contingencies were applied to incorrect responses. In the Pavlovian-only trials, presentation of a fractal cue was directly followed by a probabilistic outcome (Figure 1B).

Downloaded from http://direct.mit.edu/jocn/article-pdf/35/12/2089/2170792/jocn_a_02062.pdf by University of Glasgow user on 05 June 2026

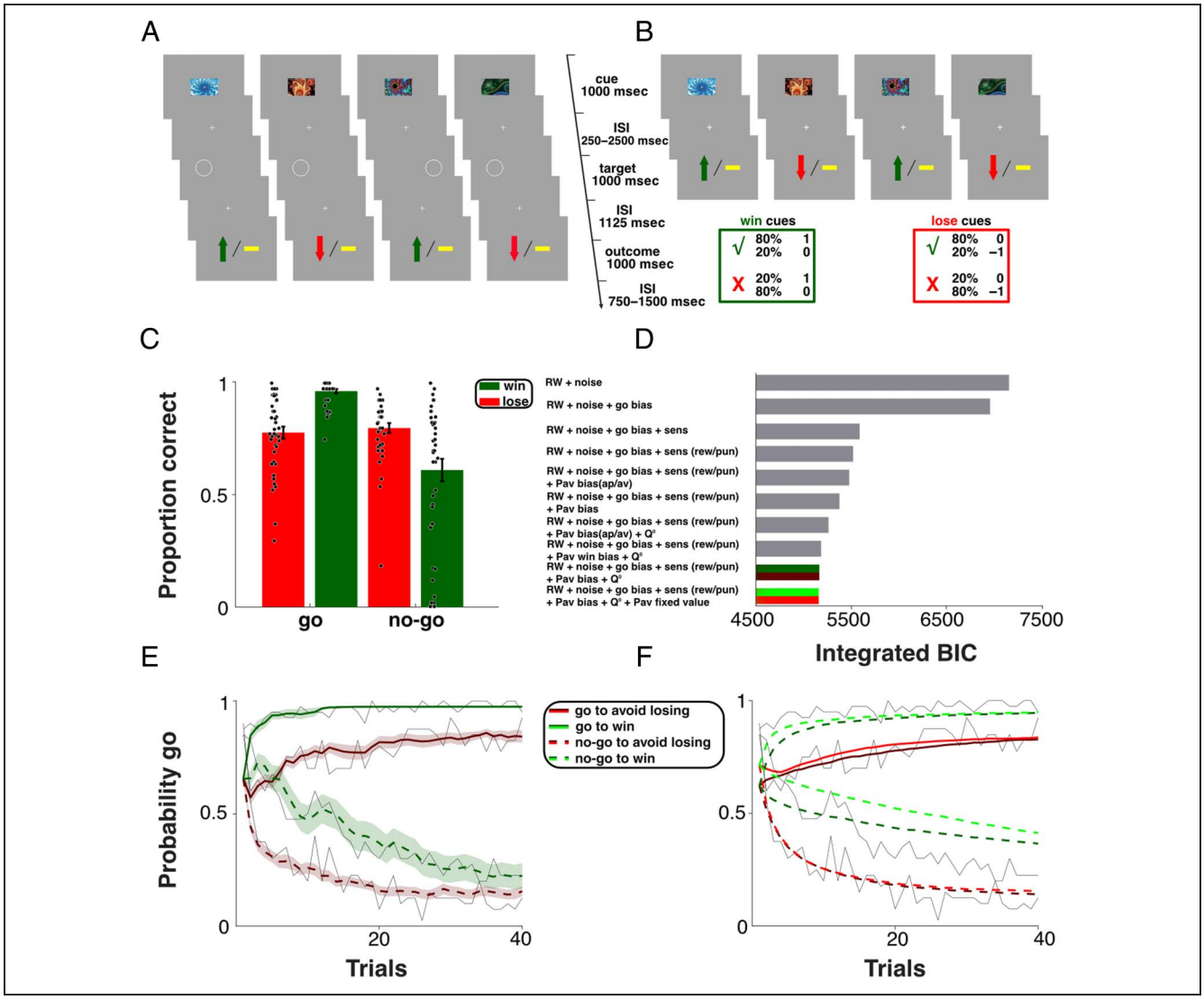

Figure 1. Task design and behavior. Mixed (A) and Pavlovian-only (B) trials. Response–outcome contingencies for win and lose cues are shown in the green and red box, respectively. (C) Proportion of correct choices as a function of action requirement and valence. Error bars denote *SEM*. (D) Predictive performance of candidate models assessed using the integrated Bayesian information criterion (BIC). Smaller values indicate better predictive performance. (E) Fitted behavioral data from the "dynamically learned" Pavlovian value model. (F) Simulated behavioral data (dark colors for the "dynamically learned" Pavlovian value model and light colors for the "fixed" Pavlovian value model). Gray lines represent observed mean choice behavior (i.e., trial-wise probability of choosing go action). Colored shadings represent *SEM*.

Outcomes were selected as if participants had made the correct response. We did not yoke outcomes in the Pavlovian-only trials to the individual win/lose outcome rates on the mixed trials so that the updating of the Pavlovian value was not tied to instrumental performance during the Pavlovian-only trials. This experimental manipulation allowed us to better decorrelate Pavlovian and instrumental predictions. Moreover, we capitalized on the trial-by-trial variability of fitted Pavlovian and instrumental predictions to enhance power to detect covarying fMRI activations. Fractal cues were counterbalanced across both mixed and Pavlovian-only trials.

Participants were instructed that, during mixed trials, correct responses could be either go or no-go. For the go responses, they were advised to press either a right or left button depending on the side of the screen the cue was shown on. They were informed of the probabilistic nature of the task and had to learn stimulus–response–outcome contingencies by trial and error. Participants were advised they could win up to £10 based on their task performance. Moreover, they were given the opportunity to practice an example block of the task outside the scanner so that they could familiarize themselves with the speed requirements of the task. The task was programmed using Presentation (Neurobehavioural Systems) stimulus delivery software.

Behavioral Analyses

For our behavioral analyses, we conducted maximal by-participant random intercept and random slopes generalized and log-linear mixed-effects models (Barr, Levy,

Downloaded from http://direct.mit.edu/jocn/article-pdf/35/12/2089/2170792/jocn_a_02062.pdf by University of Glasgow user on 05 June 2026

Scheepers, & Tily, 2013) using the *lme4* package in R (www.r-project.org) and allowing for random correlations between independent variables. We tested the statistical significance of the fixed effects using the likelihood ratio test (Barr et al., 2013). Moreover, in the presence of an interaction between a factorial predictor and a continuous covariate, we derived estimates of the covariate slopes for each level of the factorial predictor and tested their statistical significance using the *emmeans* package in R. We dealt with nonconvergence issues because of model singularity (or near-singularity) by dropping terms in the random effects structure of the model.

To test task-related learning effects as a function of task block, valence, and action requirement, we conducted the following mixed-effects regression model:

$$\begin{aligned} logit(Accuracy) &= 1 + Block + Valence * Action \\ &+ (1 + Block + Valence * Action | Subject) \end{aligned}$$

To further assess behavioral effects of motivational biases, we regressed valence and accuracy on RTs as per the following model:

$$\begin{aligned} \log(RT) &= 1 + Valence * Accuracy \\ &+ (1 + Valence * Accuracy | Subject) \end{aligned}$$

Computational Modeling of Behavioral Data

We fitted a nested sequence of differently parameterized RL models. On each trial t, action weight W represented the expected value assigned to go and no-go responses for a given cue i and determined propensity p for action $a \in \{go, no-go\}$ according to the following decision function:

$$p\left(a^t_{go} | cue^t_i\right) = \sigma\left(\left(W^t_{go} | cue^t_i\right) - \left(W^t_{no-go} \middle| cue^t_i\right)\right)(1 - noise) + \frac{noise}{2}$$

where $\sigma()$ is a standard sigmoid function and noise is a free parameter that can vary between 0 and 1. The expected value Q for instrumental actions was updated according to a Rescorla-Wagner (RW) learning rule parameterized as follows:

$$\begin{aligned} Q^t_i\left(a^t | cue^t_i\right) &= Q^{t-1}_i\left(a^{t-1} | cue^{t-1}_i\right) \\ &+ \alpha\left(\rho r^t - Q^{t-1}_i\left(a^{t-1} | cue^{t-1}_i\right)\right) \end{aligned}$$

where $r^t \in \{1, 0, -1\}$ represents the outcome, α is the learning rate, and ρ is an outcome sensitivity parameter. Whereas in the base model RW (learning rate + noise), we did not include a sensitivity parameter, in other model parameterizations, we included either a single sensitivity parameter ρ for both reward and punishment or two distinct sensitivity parameters allowing for differential scaling of reward (ρ_rew) and punishment (ρ_pun) outcomes. To account for the observed tendency to favor go over no-go responses, especially in the early trials of the task, we incorporated a time-invariant, fixed, go bias parameter b into action weight W as follows:

$$W^t_i\left(a^t | cue^t_i\right) \begin{cases} Q^t_i\left(a^t | cue^t_i\right) + b \text{ if } a^t = \text{go} \\ Q^t_i\left(a^t | cue^t_i\right) \quad \text{else} \end{cases}$$

We also allowed for the initial instrumental value Q^0 of all cues to be a free parameter; otherwise, we set it to 0. The initial Pavlovian value V^0 of all cues was set to 0. To estimate the biasing effect of the Pavlovian system over instrumental learning, we integrated Pavlovian expected value V in the update equation of action weight W as follows:

$$W^t_i\left(a^t | cue^t_i\right) \begin{cases} Q^t_i\left(a^t | cue^t_i\right) + b + \pi V^t_i\left(cue^t_i\right) \text{ if } a = \text{go} \\ Q^t_i\left(a^t | cue^t_i\right) \quad \text{else} \end{cases}$$

where π is a free parameter indexing the magnitude of Pavlovian bias (the greater π, the greater the influence of the Pavlovian system on instrumental responding). The Pavlovian expected value V was updated according to the following equation:

$$V^t_i\left(cue^t_i\right) = V^{t-1}_i\left(cue^{t-1}_i\right) + \alpha\left(\rho r^t - V^{t-1}_i\left(cue^{t-1}_i\right)\right)$$

Given that the sign of the Pavlovian expected value V depended on the valence of each cue (i.e., positive for win cues and negative for lose cues), V enhanced instrumental responding by increasing the value of the go action during the win trials. Conversely, V disrupted instrumental responding by decreasing the value of the go action during the lose trials. Moreover, in a further variant of the model, we employed two different Pavlovian biases π (approach and avoidance) to estimate the differential effect of Pavlovian invigoration (π_app) and suppression (π_avd) on go responses. Finally, we tested the additional hypotheses that (i) the Pavlovian biasing of the go action was restricted to the win trials and (ii) a static (as opposed to a dynamically learned) Pavlovian value (ψ), which can only be inferred upon the first nonneutral outcome, contributed to the action weights (Swart et al., 2018). To preserve the parameters' natural bounds, log (ρ, π, ψ) and logit ($noise, \alpha$) transforms of the parameters were implemented. We set the initial value of the free parameters' ($noise, \alpha, b, \rho, \rho_{rew}, \rho_{pun}, \pi, \pi_{app}, \pi_{avd}, Q^0, \psi$) prior means in their native space to (0.5,0.5,0,1,1,1,1,1,1,0,1) and their prior variances to 100.

Importantly, although updating of Pavlovian value in the absence of any instrumental learning during the Pavlovian-only trials enabled partial decorrelation of Pavlovian and instrumental value estimates, Pavlovian learning was still tied to instrumental performance during mixed trials.

Model Fitting and Validation

To compute parameter estimates, we implemented a Type II maximum likelihood fitting procedure as previously described in Huys et al. (2011). We optimized the log likelihood of observed data Y by performing k iterations of an

Downloaded from http://direct.mit.edu/jocn/article-pdf/35/12/2089/2170792/jocn_a_02062.pdf by University of Glasgow user on 05 June 2026

expectation–maximization routine until convergence. Briefly, at each iteration k, in the expectation step, we optimized the log likelihood with respect to the distribution over the parameters θ holding prior parameters η fixed:

$$q^k(\theta) = p\left(\theta|Y, \eta^{k-1}\right)$$

We used the Laplace approximation for $q^k(\theta) \sim N = (m^k, s^k)$ and for each participant i, updated the mean m and variance s of the normal distribution as follows:

$$m_i^k = \underset{\theta}{argmax}\ p\left(Y_i, \theta_i|\eta^{k-1}\right)$$

$$s_i^k = \left(\frac{\partial^2 p\left(Y_i, \theta_i|\eta^{k-1}\right)}{\partial\theta_i^2}\Big|_{\theta_i = m_i^k}\right)^{-1}$$

Subsequently, in the maximization step, we optimized the log likelihood with respect to prior parameters η holding the distribution over the parameters θ fixed:

$$\eta_m^k = \frac{1}{N}\sum_i^N m_i^k$$

$$\eta_s^k = \frac{1}{N}\sum_i^N \left(m_i^k\right)^2 + s_i^k - \eta_m^k$$

The advantage of this hierarchical approach was to prevent overfitting and avoid noisy parameter estimates because poorly constrained parameters were regularized by prior parameters.

We estimated the log-likelihood as the cross-entropy loss function:

$$\sum^N y log\hat{y} + (1-y)\log(1-\hat{y})$$

where y and ŷ represent observed and predicted choices, respectively.

To verify the model's goodness of fit, we computed the 20% bend correlation coefficient between observed and model-predicted group-level trial-wise probabilities of go action. Furthermore, we performed parameter recovery and thus tested whether parameters of the best-fitting model were identifiable. We simulated new data using fitted parameters and estimated parameters again on simulated data. Subsequently, we computed the 20% bend correlation coefficient between true and recovered parameters.

Model Comparison and Model Falsification

To select the best-fitting model, we evaluated both predictive and generative performance of the candidate models (Palminteri, Wyart, & Koechlin, 2017). We initially performed model comparison by estimating the group-level BIC_{int} for N individuals as described in Huys et al. (2011). Briefly, to estimate the log model evidence $p(Y|\ \eta)$, we approximated the integral over the parameters by sampling θ from the prior distribution $N(\eta_m, \eta_s)$ 1000 times:

$$\int logp(Y|\theta)logp(\theta|\eta)d\theta \sim \frac{1}{K}\sum^K logp\left(Y|\hat{\theta}\right)$$

$$BIC_{int} = \sum^N logp\left(Y|\hat{\theta}\right) - \frac{1}{2}|\theta|\log|Y|$$

where $\hat{\theta}$ is the sampled parameters, $|\theta|$ is the number of parameters in the model, and $|Y|$ is the number of data points. The BIC_{int} represents a parsimonious estimate of a model's goodness-of-fit based on both optimized parameters and hyperparameters. Nonetheless, the BIC_{int} is a relative measure of a model's goodness-of-fit and only provides information on whether a given model outperforms competing modeling hypotheses.

To assess generative performance, we subsequently simulated behavioral data and compared observed and simulated trial- and cue-wise group-level probabilities of the go action. To generate surrogate behavioral data, we played the task 100 times resampling fitted parameters without replacement. We stochastically determined action using model-derived choice propensities and randomly selected outcomes according to the ground-truth feedback schedule. We then averaged group-level trial-wise probabilities of the go action and correlated it with observed probability of the go action using 20% bend correlation test.

fMRI Data Acquisition

We used a 3-T TIM Trio MRI scanner (Siemens) with a 12-channel head coil to record MRI data. Cushions were placed around the head to minimize head motion. We acquired a high-resolution T1-weighted structural image (1-mm isotropic voxels, 128 axial slices, inversion time = 900 msec, repetition time [TR] = 2300 msec, echo time [TE] = 2.96 msec, flip angle = 90°), a T2*-weighted EPI functional scan (2-mm isotropic voxels, 68 axial slices, TR = 2000 msec, TE = 26 msec, flip angle = 60°) using Multiband 2 acquisition, phase, and magnitude field maps (3.3 × 3.3 × 3 mm voxels, 46 axial slices, TR = 488 msec, short TE = 4.92 msec, long TE = 7.38 msec) for distortion correction of the acquired EPI images (Weiskopf, Hutton, Josephs, & Deichmann, 2006). Slice orientation was tilted +30° from the AC–PC plane to reduce susceptibility-induced signal dropout (Weiskopf et al., 2006).

fMRI Data Preprocessing and Analysis

MRI data were preprocessed and analyzed using FSL software (Smith et al., 2004). The preprocessing pipeline involved B0 unwrapping (Jenkinson, 2003), intramodal motion correction using MCFLIRT (Jenkinson, Bannister, Brady, & Smith, 2002), slice timing correction, spatial smoothing with an isotropic 5-mm FWHM Gaussian

Downloaded from http://direct.mit.edu/jocn/article-pdf/35/12/2089/2170792/jocn_a_02062.pdf by University of Glasgow user on 05 June 2026

kernel, and high-pass temporal filtering with 110 sec. Cut-off frequency and grand-mean intensity normalization of each entire 4-D data set. EPI scans were subsequently co-registered with skull-stripped structural images using boundary-based registration (FLIRT; Greve & Fischl, 2009; Jenkinson & Smith, 2001) and spatially normalized into Montreal Neurological Institute (MNI) 152 space using FNIRT nonlinear registration.

fMRI Data Analysis

We performed whole-brain statistical analyses of fMRI data using a multilevel mixed-effects approach as implemented in FLAME 1 + 2 (FSL; Beckmann, Jenkinson, & Smith, 2003). Regressors were convolved with a double-gamma hemodynamic response function. Six additional motion parameters (three translations and three rotations) estimated during the motion correction phase were included in the design matrix as regressors of no interest. We used FSL collinearity diagnostics to ensure design matrices were well conditioned and not rank deficient. At the first level, we estimated contrasts of the parameter estimates specified in the design matrix. At the second and third level, we conducted a one-sample t test of the lower-level contrasts of the parameter estimates to account for between-blocks (second level) and between-participant (third level) random effects. We thresholded Z statistic images using a cluster-defining threshold of $Z > 3.1$ and an FWE-corrected significance threshold of $p = .05$.

To elucidate the neural circuitry underpinning Pavlovian and instrumental valuation systems and PII effects, we performed two sets of fMRI analyses: *task-informed* and *model-informed* analyses. Whereas in the task-informed approach, we built a general linear model (GLM) using only task events, in the model-informed approach, we built regressors from the Pavlovian and instrumental value estimates (and their respective prediction errors) of our winning computational model fit. The goals of the model-informed fMRI analyses were (i) to validate modeling results and (ii) to uncover parametric hemodynamic responses associated with instrumental and Pavlovian predictions and PII effects.

Task-informed GLM

The regressors of interest in the design matrix were four unmodulated boxcar functions, each aligned with and lasting for the duration of the cue presentation. Moreover, nuisance regressors included two boxcar regressors modeling response-time modulated go and unmodulated no-go responses in the target detection phase, one modulated boxcar regressor modeling outcome (i.e., +1 for rewards, 0 for neutral outcomes, and −1 for punishments), and one unmodulated regressor modeling late response trials. We then used the parameter estimates of the cue-wise regressors to set up linear contrasts designed to capture main effects of action requirement (go vs. no-go cues), inaction (no-go vs. go cues), positive valence (win vs. lose cues), negative valence (lose vs. win cues), congruence (congruent vs. incongruent cues), and incongruence (incongruent vs. congruent cues).

Model-informed GLM

In this fMRI analysis, we capitalized on the results of computational modeling and constructed a GLM to investigate the main effects of instrumental and Pavlovian value expectations and PII effects. We modeled the cue presentation phase of the task by building two parametric regressors encoding the instrumental value of action (i.e., Q_{go}–$Q_{no\text{-}go}$) associated with the presented cue (instrumental regressor) and its motivational value (Pavlovian regressor). It is important to note that the linear (positive) contrast of the instrumental regressor is action specific as it captures differential hemodynamic responses to the go action value compared to the no-go action value (and vice versa with the negative contrast). We modeled PII effects by means of a third regressor representing the element-wise product of the magnitude of the instrumental and Pavlovian regressors. The resulting signed interaction regressor was positive in the case of congruent (i.e., same-sign) instrumental and Pavlovian regressors and negative in the case of incongruent (i.e., different-sign) instrumental and Pavlovian regressors. We conducted a positive and negative linear contrast of the interaction regressor to uncover synergistic (positive contrast) versus antagonistic (negative contrast) PII neural effects over and above Pavlovian and instrumental main effects. It is important to note that our interaction regressor conflated cooperation (and competition) interaction effects across appetitive and aversive domains. Notably, we orthogonalized the PII regressor with respect to the instrumental and Pavlovian regressors. In the outcome phase, we built two parametric regressors encoding instrumental and Pavlovian prediction errors. As in the task-informed GLM, we also included nuisance regressors accounting for visual stimulation in the decision and outcome phases, go and no-go responses in the target decision phase, and late response trials. Moreover, we performed a supplementary analysis where we included a nuisance modulated regressor (i.e., +1 for go and −1 for no-go responses) modeling motor response in the cue presentation phase. The purpose of this analysis was to control for any confounding effects of preparatory motor activity pertaining to the encoding of the instrumental value of action. Although in all GLMs, we modeled the outcome phase, the design of the task was optimized to uncover hemodynamic responses to cue presentation. We therefore focused our analysis on the presentation phase and only discuss findings pertaining to it.

We also conducted ROI analyses based on previous findings in the literature implicating the striatum and inferior frontal gyrus (IFG) in instrumental and Pavlovian learning (Guitart-Masip, Chowdhury et al., 2012; Guitart-Masip, Huys et al., 2012; Guitart-Masip, Fuentemilla et al.,

Downloaded from http://direct.mit.edu/jocn/article-pdf/35/12/2089/2170792/jocn_a_02062.pdf by University of Glasgow user on 05 June 2026

2011). Using FLS's Harvard–Oxford cortical and subcortical structural atlases, we created anatomical masks of the striatum and IFG, thresholded at 50%, and used them to mask second-level contrast images of interest, which we then entered into a third-level one-sample t test where we performed cluster-level inference as in the whole-brain analyses.

Time Course Analysis of fMRI Data

We conducted follow-up analyses, and for each participant, we extracted BOLD signal time courses from the FWE-corrected significant clusters identified by the model-informed GLM and therefore encoding instrumental and Pavlovian expected value and PII effects. The aim of these follow-up analyses was threefold: (i) to visualize cluster-wise valence/action/congruence effects, (ii) to correlate cluster-wise mean activity with subject-wise behavioral performance, and (iii) to predict trial-by-trial individual behavior (i.e., choice accuracy and RTs). For these analyses, we reverse normalized masked clusters of interest from standard into functional space to retrieve cluster- and trial-wise BOLD activity from participant-specific preprocessed functional scans. We then estimated cluster-wise BOLD percentage signal change traces locked to the onset of the decision phase for all events of interest as follows (Philiastides, Biele, & Heekeren, 2010):

$$\text{BOLD\%signal change}_j^t = \left(\frac{\text{BOLD}_j^t - \text{BOLD baseline}_j}{\overline{\text{BOLD}}}\right)$$

where j and t index trial and time point, respectively; BOLD baseline is defined as the average BOLD signal over the 4 sec preceding the event of interest; and $\overline{\text{BOLD}}$ is the mean BOLD signal across all time points. To ascertain brain–behavior correlations, we performed 20% bend correlation between the subject-wise, cue-locked mean BOLD signal change averaged over a time window of interest and individual mean behavioral performance. To avoid erroneous inferences (also known as the interaction fallacy; Nieuwenhuis, Forstmann, & Wagenmakers, 2011), we compared nonoverlapping dependent correlation coefficients using percentile bootstrap (Wilcox, 2016). To predict trial-by-trial behavior, we conducted single-trial regression of cluster-wise peak BOLD activity against choice accuracy and RT using the following mixed-effects models and dropping terms from the random effects in case of model singularity or near-singularity:

$$\text{logit(Accuracy)} = 1 + \text{BOLD} * \text{cue} + (1 + \text{cue}|\text{Subject})$$

$$\log(\text{RT}) = 1 + \text{BOLD} + (1 + \text{BOLD}|\text{Subject})$$

RESULTS

Behavioral Asymmetries as a Function of Conflicting Pavlovian and Instrumental Effects

The well-documented disrupting interference of motivational biases with instrumental responding was borne out by behavioral evidence that, on average, task performance was greater for congruent (go to win: 96 ± 5%; no-go to avoid losing: 79 ± 14%) than incongruent (go to avoid losing: 77 ± 17%; no-go to win: 61 ± 31%) cues (Figure 1C). Correspondingly, there was a statistically significant effect of congruence (i.e., Action × Valence interaction), $\chi^2(1) = 29.2, p < .001$, on choice accuracy. Moreover, we found evidence for both valence-dependent and action-dependent behavioral biases as confirmed by significant valence-adjusted main effect of action, $\chi^2(1) = 14.4, p < .001$, and action-adjusted main effect of valence, $\chi^2(1) = 12, p < .001$, on choice accuracy. In summary, participants performed better in response to (i) go compared to no-go cues, (ii) win compared to lose cues, and (iii) congruent compared to incongruent cues.

Importantly, there was evidence that, on average, participants successfully learned cue–response contingencies. Indeed, mean performance improved over the course of the task as shown in Figure 2A and as confirmed by the finding of a significant effect of task block on choice accuracy, $\chi^2(1) = 26.6, p < .001$.

Cue valence influenced speed of RTs (Figure 2B). Participants responded faster after win (mean = 0.436 sec, $SEM = 0.08$) compared to lose (mean = 0.448 sec, $SEM = 0.08$) cues. Whereas the valence-adjusted main effect of accuracy was statistically significant, $\chi^2(1) = 9.35, p = .002$, the accuracy-adjusted main effect of valence just fell short of statistical significance, $\chi^2(1) = 3.06, p = .057$, and the Valence × Accuracy interaction term was not significant, $\chi^2(1) = 2.78, p = .095$. For this analysis, we also included late trials as we reasoned late responses would reflect valence behavioral effect.

Overall, behavioral results revealed the presence of motivational and action-dependent learning biases in accordance with the two-process theory of associative learning, which postulates the coexistence of Pavlovian and instrumental systems during learning.

Computational Modeling Corroborates Pavlovian Biasing of Instrumental Learning

We found that although the predictive performance of the "dynamically learned" Pavlovian value model ($\text{BIC}_i = 5167$) was worse than that of the "fixed" Pavlovian value model ($\text{BIC}_i = 5160$; Figure 1D), its generative performance was better (Figure 1F), especially regarding the no-go to win condition. To objectively evaluate generative performance, we estimated the mean squared error (MSE) between simulated and observed mean choice behavior for both models. We found that the "dynamically learned" Pavlovian value model ($MSE = 1.18$) better reproduced

Downloaded from http://direct.mit.edu/jocn/article-pdf/35/12/2089/2170792/jocn_a_02062.pdf by University of Glasgow user on 05 June 2026

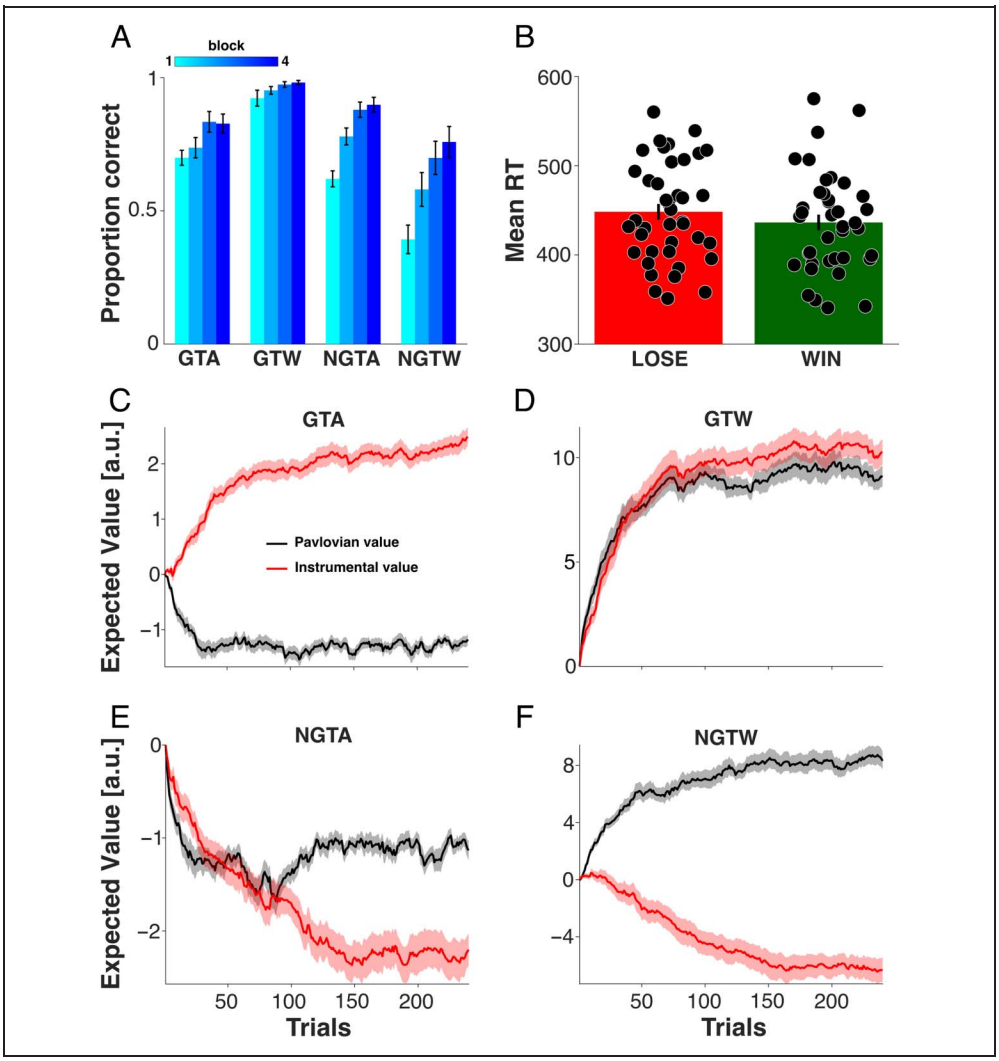

Figure 2. (A) Proportion of correct choices as a function of action requirement, valence, and task block (n = 4). GTA = go to avoid losing; GTW = go to win; NGTA = no-go to avoid losing; NGTW = no-go to win. Error bars denote *SEM*. (B) Mean of median RTs in milliseconds for lose (red bar) and win (green bar) conditions showing valence effect on speed of responding. Error bars denote *SEM*. Black dots represent individual participants. (C–F) Trial-by-trial trace plots of cue-wise fitted instrumental and Pavlovian expected value. Solid color-coded lines denote mean expected value and colored shadings represent *SEM*. At the population level, the Pavlovian and instrumental regressors were only partially correlated (Pearson's rho = 0.36).

observed behavioral effects than the "fixed" Pavlovian value model (*MSE* = 1.54; Figure 1F). To thus arbitrate between these two models, we reasoned that generative performance should be given more weight because it represents an "absolute" rather than "relative" model comparison criterion and the ability to reproduce behavioral effects of interest is a critical aspect of model validation (Palminteri et al., 2017).

Crucially, fitted, $r_{\text{bend}}(158) = .98, p < .001$, and simulated, $r_{\text{bend}}(158) = .97, p < .001$, data of the "dynamically learned" Pavlovian value model provided a good fit to observed choice behavior (Figure 1E and F). Finally, we were able to successfully recover fitted parameters using our hierarchical Type II maximum likelihood fitting routine (noise: $r_{\text{bend}}(38) = .36, p = .02$; α: $r_{\text{bend}}(38) = .80$, $p < .001$; b: $r_{\text{bend}}(38) = .71, p < .001$; ρ_{rew}: $r_{\text{bend}}(38) = .45$, $p = .003$; ρ_{pun}: $r_{\text{bend}}(38) = .60$, $p < .001$; π: $r_{\text{bend}}(38) = .72, p < .001$; Q^0: $r_{\text{bend}}(38) = .86, p < .001$).

Our modeling results replicated evidence from previous modeling work denoting Pavlovian biasing of actions (Ousdal et al., 2018; Swart et al., 2018; Mkrtchian, Aylward, Dayan, Roiser, & Robinson, 2017; Swart et al., 2017; Guitart-Masip, Huys et al., 2012) and are concordant with the observed asymmetries in behavioral performance. Interestingly, unlike previous work (Mkrtchian et al., 2017), albeit using a different experimental setting, we found that accounting for differential effects (i.e., approach vs. avoidance) of the Pavlovian expected value on the action weight did not significantly improve model parsimony. It is possible that, in previous work, the threat posed by unpredictable electric shocks may have increased the variance of the differential Pavlovian effects on go responding.

Instrumental Value and Action Are Represented in the Action Space

In accordance with previous work (Wunderlich, Rangel, & O'Doherty, 2009), converging results from our fMRI analyses revealed instrumental value and action to be represented in the action space. The task-informed approach revealed a main effect of action (i.e., go > no-go cues) in the bilateral SMC (peak Z score = 5.09; MNI space coordinates = 8, −4, 64; $p < .05$ FWE), the precentral gyri

Downloaded from http://direct.mit.edu/jocn/article-pdf/35/12/2089/2170792/jocn_a_02062.pdf by University of Glasgow user on 05 June 2026

(right: peak Z score = 4.62; MNI space coordinates = 40, −10, 56; $p < .05$ FWE; left: peak Z score = 4.67; MNI space coordinates = −24, −4, 48; $p < .05$ FWE), and the right postcentral gyrus (peak Z score = 4.2; MNI space coordinates = 50, −18, 46; $p < .05$ FWE; Figure 6A). Conversely, the main effect of inaction (i.e., no-go > go cues) was significantly associated with a distributed group of clusters including the bilateral medial superior frontal gyrus/paracingulate gyrus (peak Z score = 4.48; MNI space coordinates = −8, 16, 66; $p < .05$ FWE), frontal pole (right: peak Z score = 4.42; MNI space coordinates = 54, 40, −6; $p < .05$ FWE; left: peak Z score = 4.46; MNI space coordinates = −24, 58, 24; $p < .05$ FWE), right IFG (peak Z score = 4.35; MNI space coordinates = 54, 18, 24; $p < .05$ FWE), and left IFG/fronto-orbital cortex (peak Z score = 4.41; MNI space coordinates = −44, 22, −10; $p < .05$ FWE; Figure 6A). A complete list of all significant clusters is provided in Table 1.

Because of the action specificity of the instrumental value positive contrast (i.e., Q_{go}–$Q_{no\text{-}go}$), we found evidence for action values in a network of areas that largely overlapped with the task-informed main effect of action, including the bilateral SMC (peak Z score = 7.79; MNI space coordinates = −6, 2, 48; $p < .05$ FWE), precentral gyri (right: peak Z score = 13.1; MNI space coordinates = 38, −10, 58; $p < .05$ FWE; left: peak Z score = 10; MNI space coordinates = −38, −12, 56; $p < .05$ FWE), left postcentral gyrus (peak Z score = 5.25; MNI space coordinates = −48, −24, 50; $p < .05$ FWE), left lateral occipital gyrus (peak Z score = 4.64; MNI space coordinates = −12, −66, 50; $p < .05$ FWE), and right cerebellum (peak Z score = 10.6; MNI space coordinates = 32, −50, −24; $p < .05$ FWE; Figure 3A). Conversely, the instrumental value negative contrast (i.e., $Q_{no\text{-}go}$–Q_{go}) revealed a cluster in the left IFG (peak Z score = 13.1; MNI space coordinates = −56, 18, 16; $p < .05$ FWE) and left superior frontal gyrus (peak Z score = 9.15; MNI space coordinates = −6, 16, 66; $p < .05$ FWE). This finding is consistent with prior evidence that greater activity in the IFG is elicited by no-go compared to go cues (Guitart-Masip, Huys et al., 2012) and that the IFG is part of a network operating as a "brake" on motor activity (Chambers et al., 2006; Figure 6E).

Contrary to previous work (Algermissen, Swart, Scheeringa, Cools, & den Ouden, 2022; Guitart-Masip, Chowdhury et al., 2012; Guitart-Masip, Huys et al., 2012; Guitart-Masip, Fuentemilla et al., 2011), we did not find evidence of a main effect of action requirement or instrumental value representations in the striatum, even when we constrained our analysis to an anatomical mask of the striatum, therefore making thresholding of statistical maps less stringent.

Instrumental Value-Related SMC Activity Correlates With Behavioral Performance in Conflict Conditions

Unsurprisingly, as we retrieved fMRI activity encoding instrumental value from the SMC and plotted mean BOLD time courses as a function of action requirement and

Table 1. Complete List of Significant fMRI Clusters for No-go > Go Contrast ($p < .05$ FEW)

	Z MAX	*MNI x*	*MNI y*	*MNI z*
Left superior frontal gyrus	4.68	8	16	66
Right frontal pole	4.42	54	40	–6
Right cuneus	4.78	4	–80	40
Right lingual gyrus	4.6	14	–52	2
Left frontal pole	4.46	–24	58	24
Right lateral occipital cortex	4.45	46	–62	32
Left frontoorbital cortex/inferior frontal gyrus	4.41	–44	22	–10
Right inferior frontal gyrus (pars opercularis)	4.35	54	18	24
Left precentral gyrus	4.06	–18	–30	60
Left central opercular cortex	4.22	–52	–10	10
Left intracalcarine cortex	4.28	–14	–66	10
Right postcentral gyrus	4.44	44	–14	36
Left cuneal cortex	4.11	–8	–88	30
Left angular gyrus	4.08	–46	–54	32
Right precentral gyrus	3.77	4	–18	62
Left precentral gyrus	4.2	–48	–12	40

MNI coordinates of maximum z statistic are shown for each cluster.

Downloaded from http://direct.mit.edu/jocn/article-pdf/35/12/2089/2170792/jocn_a_02062.pdf by University of Glasgow user on 05 June 2026

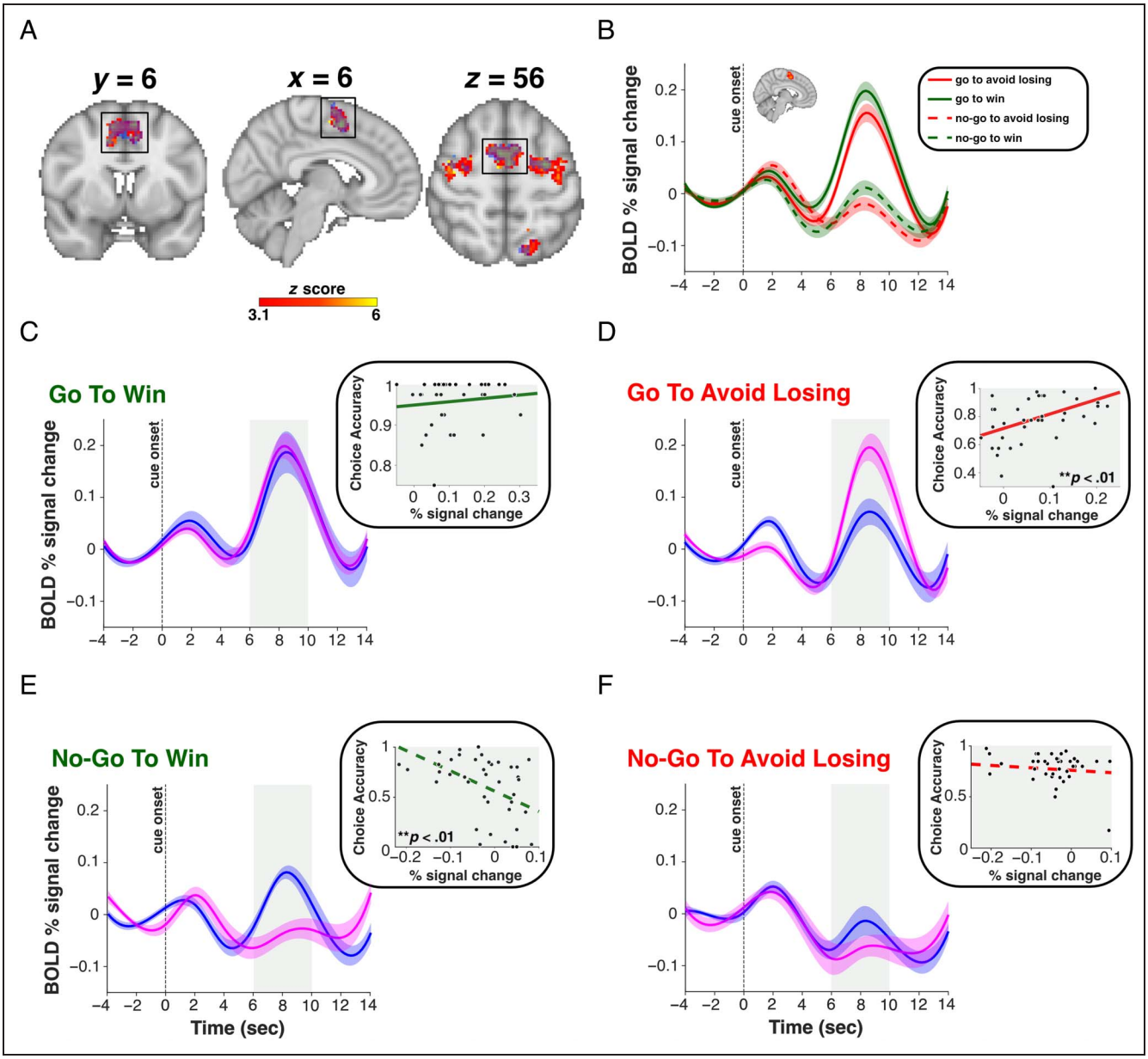

Figure 3. Neural correlates of instrumental value. (A) fMRI clusters for instrumental value with (overlaid blue–light blue shading) and without (red–yellow cluster) accounting for motor confounds ($p < .05$ FWE). SMC is highlighted by black boxes. MNI coordinates are shown. (B) BOLD traces extracted from the SMC and locked to cue onset as a function of action requirement and valence. Hemodynamic activity shows noticeable action effect (go > no-go cues). (C–F) The insets show the scatterplots of cue-wise SMC BOLD activity (averaged over the transparent gray time window shown in the BOLD traces) as a function of cue-wise choice accuracy, with color-coded lines denoting 20% bend correlation fit. Black dots represent individual participants. Notably, mean SMC hemodynamic responses to incongruent cues are significantly associated with task performance (even when accounting for motor confounds). BOLD traces represent participants in the top (purple solid lines) and bottom (blue solid lines) quartiles of choice accuracy.

valence, we observed a clear action effect in this region (Figure 3B). We then assessed the relationship between SMC activity during mixed trials and accuracy of action selection by correlating mean BOLD signal change averaged over a time window capturing surge response with individual cue-wise performance. Interestingly, we found that upregulating SMC activity in response to incongruent aversive cues (go to avoid losing: $r_{\text{bend}}(38) = .47$, $p = .002$) but downregulating it in response to incongruent appetitive cues (no-go to win: $r_{\text{bend}}(38) = -.48$, $p = .002$) correlated with greater accuracy of instrumental responding (Figure 3D and E). Conversely, although SMC hemodynamic responses to congruent cues were consistent with action requirements (i.e., increased and diminished signal change for go to win and no-go to avoid losing cues, respectively), they did not account for interindividual differences in choice accuracy (go to win: $r_{\text{bend}}(38) = .12$, $p = .47$; no-go to avoid losing: $r_{\text{bend}}(38) = -.11$, $p = .48$l Figure 3C and F). Notably, even after controlling for the potentially confounding effect of preparatory motor activity on the encoding of instrumental value, we found BOLD activity in the SMC to significantly covary with

Downloaded from http://direct.mit.edu/jocn/article-pdf/35/12/2089/2170792/jocn_a_02062.pdf by University of Glasgow user on 05 June 2026

positive instrumental value (i.e., Q_{go}–$Q_{no\text{-}go}$; peak Z score = 7.45; MNI space coordinates = 6, −4, 54; $p < .05$ FWE; Figure 3A) and to be correlated with task performance associated with incongruent (go to avoid losing: $r_{bend}(38) = .45$, $p = .003$; no-go to win: $r_{bend}(38) = -.49$, $p = .001$) but not congruent (go to win: $r_{bend}(38) = .08$, $p = .62$; no-go to avoid losing: $r_{bend}(38) = -.12$, $p = .47$) cues. It is however still possible that BOLD percentage signal change captured motor activity because (i) the SMC is recruited in the context of movement (or inhibition of action; Nachev, Kennard, & Husain, 2008) and (ii) the ISI between the cue presentation and target detection phases ranged from 250 to 2500 msec. We thus capitalized on the presence of Pavlovian-only trials (see Figure 1B) in our task where there is no target detection phase, and thus, no overt motor actions are initiated. If SMC activity in our original analysis was driven primarily by movement or action inhibition, we would expect it to dissipate in the Pavlovian-only trials. Yet, consistent with our original analysis, we still found BOLD activity in the SMC to be correlated with task performance in incongruent (go to avoid losing: $r_{bend}(38) = .34$, $p = .03$; no-go to win: $r_{bend}(38) = -.38$, $p = .017$) but not congruent (go to win: $r_{bend}(38) = .13$, $p = .43$; no-go to avoid losing: $r_{bend}(38) = -.09$, $p = .59$) trials.

We did not find any significant BOLD–behavior correlations between fMRI activity recorded in the left IFG and task performance (go to avoid losing: $r_{bend}(38) = .03$, $p = .85$; no-go to win: $r_{bend}(38) = -.013$, $p = .93$; go to win: $r_{bend}(38) = .016$, $p = .92$; no-go to avoid losing: $r_{bend}(38) = -.2$, $p = .21$).

Altogether, these results suggested that differential recruitment of the SMC during conflict conditions facilitates instrumental responding. Correspondingly, it has been documented the SMC plays a key role in successful conflict monitoring and resolution (Aron, Behrens, Smith, Frank, & Poldrack, 2007; Nachev, Rees, Parton, Kennard, & Husain, 2005). Notably, a recent imaging study reported increased hemodynamic activity in the SMC for incongruent compared to congruent cues (Algermissen et al., 2022).

Instrumental Value-related SMC Activity Predicts Trial-by-Trial RT and Choice Accuracy

On the basis of the observation that, on average, participants successfully learned cue–response contingencies, meaning that instrumental predictions effectively guided action selection, we reasoned that hemodynamic activity encoding instrumental value would be predictive of choice behavior. To this end, we regressed cue-locked peak BOLD activity in the SMC on trial-by-trial response accuracy. As we then assessed the hemodynamic effects of each cue on instrumental responding, we found that although greater BOLD activity significantly predicted greater choice accuracy for the go cues (go to avoid losing: $\beta = 1.12$, $p < .001$; go to win: $\beta = .82$, $p < .001$), the reverse was the case for the no-go cues (no-go to avoid losing: $\beta = -.94$, $p < .001$; no-go to win: $\beta = -1.10$, $p < .001$), even after accounting for motor confounds. Moreover, greater peak BOLD activity in the SMC significantly predicted faster button presses ($\beta = -.06$, $p = .004$). Taken together, these findings consolidate the role of the SMC as a critical region to implement instrumental control of behavior.

Pavlovian Value Is Encoded in the vmPFC

Surprisingly, in the task-informed fMRI analysis, we found a main effect of positive valence (i.e., win > lose cues) in the left precentral gyrus (peak Z score = 4.64; MNI space coordinates = −22, −10, 64; $p < .05$ FWE; Figure 6B) and of negative valence (i.e., lose > win cues) in the left medial caudate/accumbens (peak Z score = 4.32; MNI space coordinates = −6, 14, −2; $p < .05$ FWE; Figure 6C). The latter cluster also significantly correlated with negative Pavlovian value when we constrained our model-informed analysis to the striatum (peak Z score = 5.13; MNI space coordinates = −8, 18, 0; $p < .05$ FWE; Figure 6F).

It is plausible that the relatively greater proportion of go responses in the win trials compared to the lose trials accounted for the observed motor preparation signal associated with positive valence. Furthermore, striatal activity in the negative valence contrast may represent an anticipatory signal of potential losses as previously documented in adults and adolescents (Bretzke et al., 2023; Beck et al., 2009) and is consistent with a similar finding in a recent fMRI study (Algermissen et al., 2022).

Notably, Pavlovian expected value was positively correlated with BOLD activity in the bilateral (but predominantly left) vmPFC (peak Z score = 8.35; MNI space coordinates = −2, 58, 2; $p < .05$ FWE; Figure 4A) and negatively correlated with the right dorsal ACC (peak Z score = 5.11; MNI space coordinates = 4, 22, 38; $p < .05$ FWE; Figure 4E). Our finding replicates recent evidence that positive and negative valence effects are encoded in the vmPFC and dorsal ACC, respectively (Algermissen et al., 2022).

Pavlovian Value-related Neural Activity Biases Behavioral Performance

By sorting hemodynamic responses in the vmPFC and dorsal ACC as a function of action requirement and valence, we uncovered a noticeable valence effect in both areas (Figure 4B and F). As we anticipated, given that the updating of Pavlovian value was tied to instrumental responding during the mixed trials, this valence effect was only marginally modulated by instrumental performance.

To ascertain whether diminished encoding of Pavlovian value in the vmPFC resulted in a lesser disrupting Pavlovian effect on instrumental responding, we correlated mean BOLD percent signal change with individual task performance as a function of congruence. There was a significant BOLD–behavior correlation only for congruent, $r_{bend}(38) = .34$, $p = .03$ (Figure 4D), but not for incongruent,

Downloaded from http://direct.mit.edu/jocn/article-pdf/35/12/2089/2170792/jocn_a_02062.pdf by University of Glasgow user on 05 June 2026

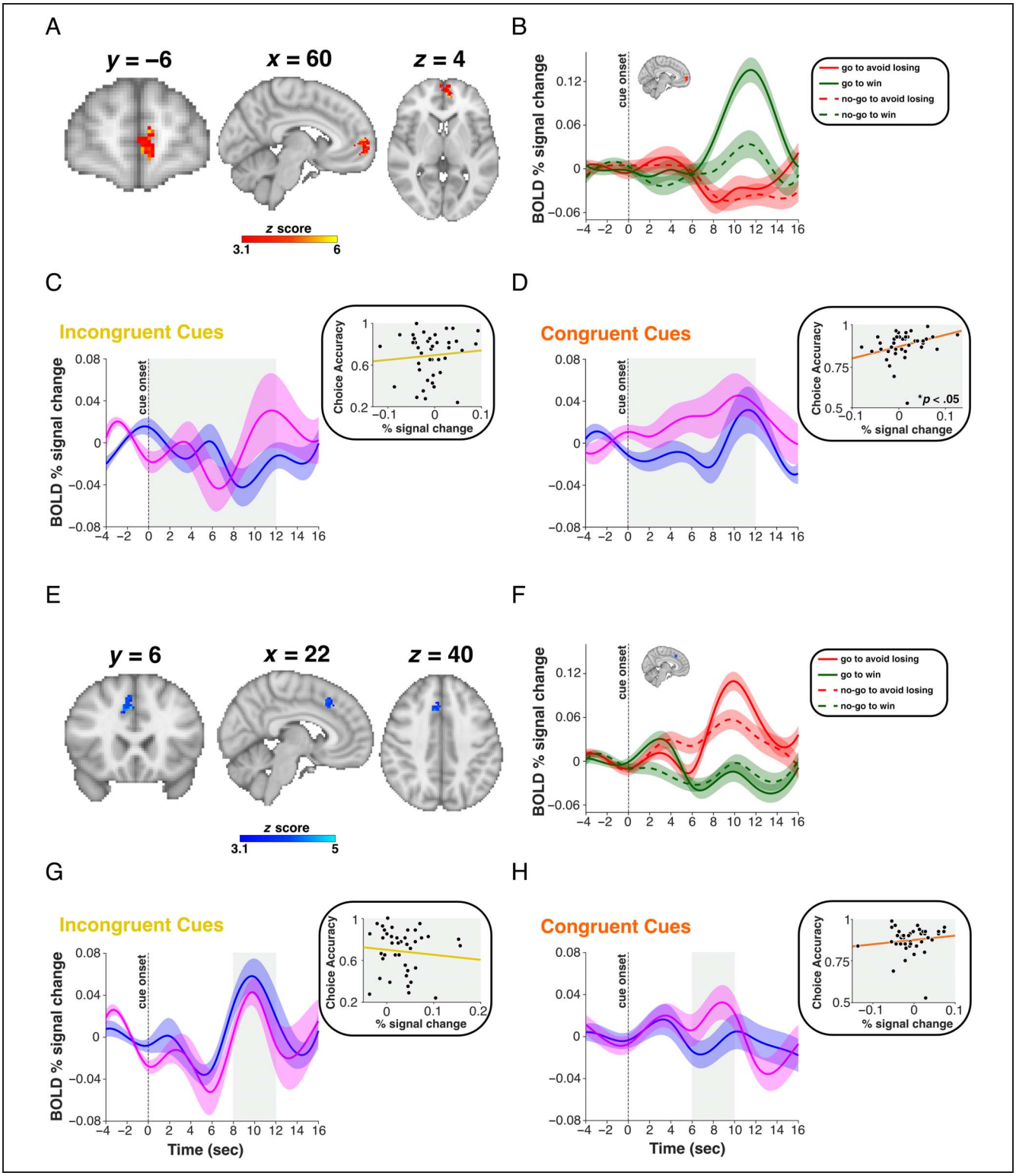

Figure 4. Neural correlates of Pavlovian value. (A) fMRI cluster in the vmPFC encoding for positive Pavlovian value ($p < .05$ FWE). MNI coordinates are shown. (B) vmPFC BOLD traces locked to cue onset as a function of action requirement and valence. Hemodynamic activity shows noticeable positive valence effect (win > lose cues). (C and D) The insets show the scatterplots of vmPFC BOLD activity (averaged over transparent gray time window shown in the BOLD traces) as a function of choice accuracy during incongruent (C) and congruent (D) trials. Notably, mean vmPFC hemodynamic responses to congruent (but not incongruent) cues are significantly associated with task performance. (E) fMRI cluster in the dorsal ACC encoding for negative Pavlovian value ($p < .05$ FWE). (F) Dorsal ACC BOLD traces locked to cue onset as a function of action requirement and valence. Hemodynamic activity shows noticeable negative valence effect (lose > win cues). (G and H) The insets show the scatterplots of dorsal ACC BOLD activity (averaged over the transparent gray time window shown in the BOLD traces) as a function of choice accuracy during incongruent (C) and congruent (D) trials. Solid color-coded lines denote 20% bend correlation fit. Black dots represent individual participants. BOLD traces represent participants in the top (purple solid lines) and bottom (blue solid lines) quartiles of choice accuracy.

Downloaded from http://direct.mit.edu/jocn/article-pdf/35/12/2089/2170792/jocn_a_02062.pdf by University of Glasgow user on 05 June 2026

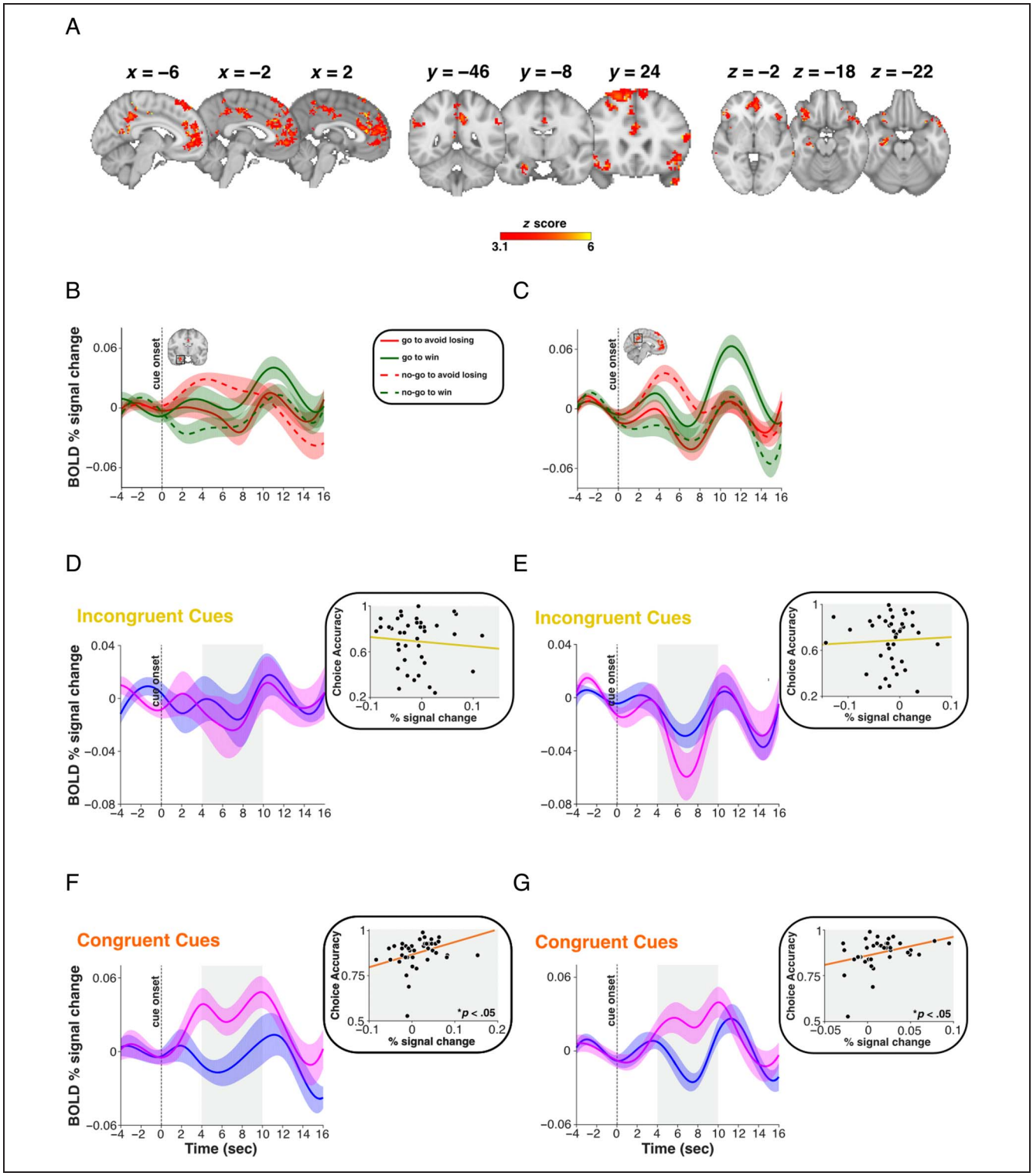

Figure 5. Neural correlates of congruent PII effects. (A) fMRI clusters encoding for appetitive and aversive congruent PII effects ($p < .05$ FWE). MNI coordinates are shown. (B and C) BOLD traces extracted from the right amygdala/hippocampus complex (B) and bilateral PCC (C) locked to cue onset as a function of action requirement and valence. Hemodynamic activity shows noticeable congruence effect (congruent > incongruent cues) with earlier peak for aversive and later peak for appetitive congruent cues. (D–G) The insets show the scatterplots of BOLD activity (averaged over the transparent gray time window shown in the BOLD traces) in the right amygdala/hippocampus complex (D/F) and bilateral PCC (E/G) as a function of choice accuracy during incongruent (D/E) and congruent (F/G) trials, with solid color-coded lines denoting 20% bend correlation fit. Black dots represent individual participants. Notably, mean hemodynamic responses to congruent (but not incongruent) cues in the right amygdala/hippocampus complex and bilateral PCC are significantly associated with task performance. BOLD traces represent participants in the top (purple solid lines) and bottom (blue solid lines) quartiles of choice accuracy.

Downloaded from http://direct.mit.edu/jocn/article-pdf/35/12/2089/2170792/jocn_a_02062.pdf by University of Glasgow user on 05 June 2026

Table 2. Complete List of Significant Clusters for Congruent Pavlovian × Instrumental Interaction Contrast ($p < .05$ FWE)

	Z MAX	*MNI x*	*MNI y*	*MNI z*
Right superior frontal gyrus	13.6	26	18	58
Left lateral occipital gyrus	14	–58	–62	18
Posterior cingulate cortex	8.33	4	–20	34
Left temporal pole	11.6	–58	8	–6
Right OFC	10.3	52	22	–10
Right angular/supramarginal gyrus	13.6	46	–50	38
Right lateral occipital gyrus	6.83	48	–68	44
Right hyppocampus/amygdala	7.36	28	–22	–16
Right precuneus	7.21	4	–52	12
Right middle temporal cortex	8.32	64	–34	–4
Left middle frontal gyrus	5.85	46	10	56

MNI coordinates of maximum z statistic are shown for each cluster.

$r_{\text{bend}}(38) = .099$, $p = .54$, cues (Figure 4C). However, when we tested for a significant interaction effect, we found that the difference between correlation coefficients was nonsignificant (r_{cong}–$r_{\text{incong}} = .25$ [−.13–.64], $p = .22$). Our findings corroborate previous evidence that optimal action selection is achieved by enhanced effort-based overriding of Pavlovian influence on behavior rather than by attenuated Pavlovian behavioral biases (Cavanagh, Eisenberg, Guitart-Masip, Huys, & Frank, 2013). Notably, peak vmPFC BOLD activity did not predict trial-by-trial choice accuracy (go to avoid losing: $\beta = .07$, $p = .55$; go to win: $\beta = .4$, $p = .08$; no-go to avoid losing: $\beta = -.05$, $p = .65$; no-go to win: $\beta = .13$, $p = .3$). Furthermore, mean BOLD activity in the dorsal ACC was not significantly correlated with performance during congruent, $r_{\text{bend}}(38) = .15$, $p = .34$, and incongruent, $r_{\text{bend}}(38) = -.09$, $p = .56$, trials (Figure 4G and H).

We then assessed the effect of motivational biases on speed of trial-by-trial responses and found that greater (peak) BOLD activity in the vmPFC and dorsal ACC sped

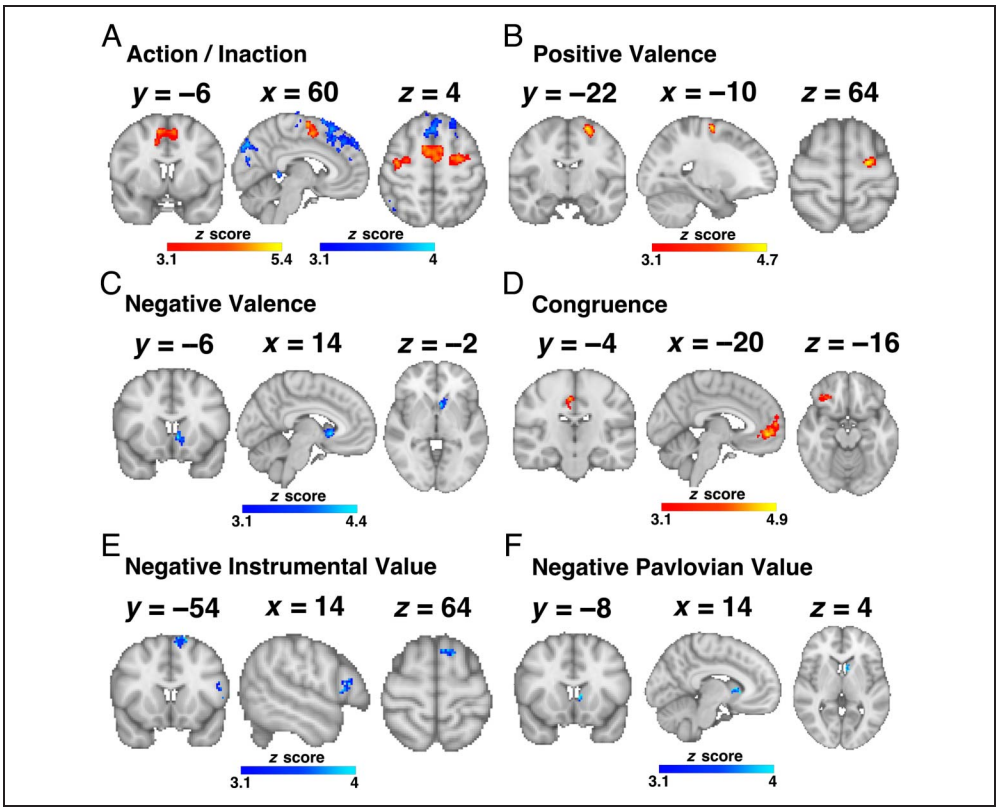

Figure 6. (A–D) Results from task-informed fMRI analysis showing significant clusters associated with action (go > no-go cues), inaction (no-go > go cues), positive valence (win > lose cues), negative valence (lose > win cues), and congruence (congruent > incongruent cues). (E and F) Results from model-informed fMRI analysis (whole-brain [E] and using an anatomical mask of the striatum [F]). A cluster in the left IFG was significantly associated with negative instrumental value (E). A cluster in the left medial caudate was significantly associated with negative Pavlovian value (F). MNI coordinates are shown.

Downloaded from http://direct.mit.edu/jocn/article-pdf/35/12/2089/2170792/jocn_a_02062.pdf by University of Glasgow user on 05 June 2026

up ($\beta = -.04, p = .021$) and slowed down ($\beta = .095, p < .001$) motor responses, respectively. Consistent with similar recent result (Algermissen et al., 2022), our findings further implicate neural activity in the vmPFC and dorsal ACC in exerting Pavlovian biases on behavior.

Synergistic Pavlovian and Instrumental Predictions Are Represented in the Limbic System and Medial pFC

The final step of our fMRI analysis was to identify neural structures encoding PII effects in both the appetitive and aversive domains (Figure 5). In the task-informed fMRI analysis, we uncovered a main effect of congruence (congruent > incongruent cues) in the bilateral vmPFC (peak Z score = 4.84; MNI space coordinates = −6, 48, −4; $p <$ .05 FWE), right frontal pole (peak Z score = 3.88; MNI space coordinates = 34, 48, 28; $p <$ .05 FWE), right OFC (peak Z score = 4.28; MNI space coordinates = 32, 32, −14; $p <$ .05 FWE), right posterior cingulated cortex (PCC; peak Z score = 4.39; MNI space coordinates = 6, −20, 46; $p <$ .05 FWE), left parietal opercular cortex (peak Z score = 4.12; MNI space coordinates = −54, −28, 26; $p <$ .05 FWE), and left superior parietal cortex (peak Z score = 4.1; MNI space coordinates = −24, −42, 56; Figure 6D). No clusters associated with a main effect of incongruence (i.e., incongruent > congruent cues) survived multiple comparison correction.

Compared to the task-informed fMRI analysis, the model-informed approach uncovered a broader network of (partially overlapping) activations in the brain (Figure 4A). When Pavlovian and instrumental value

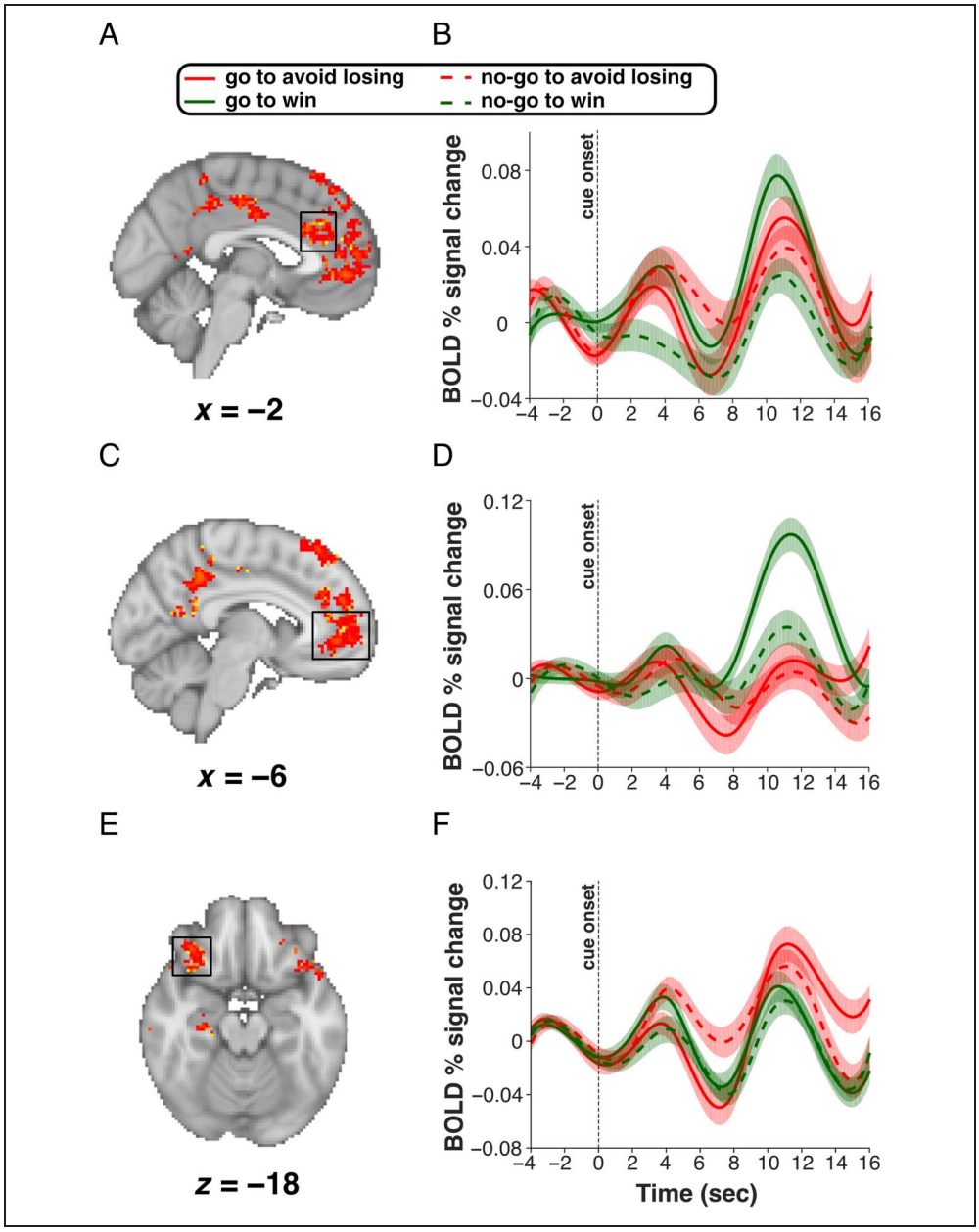

Figure 7. fMRI clusters encoding for appetitive and aversive congruent PII effects ($p <$ .05 FWE) and BOLD traces locked to cue onset as a function of action requirement and valence. MNI coordinates are shown. (A and B) Dorsal ACC. (C and D) Bilateral medial pFC. Congruence effect is primarily driven by go to win cues. (E and F) Right OFC.

Downloaded from http://direct.mit.edu/jocn/article-pdf/35/12/2089/2170792/jocn_a_02062.pdf by University of Glasgow user on 05 June 2026

expectations converged, we detected significant BOLD activity in regions pertaining to the limbic system such as the bilateral perigenual ACC/medial pFC (peak Z score = 10.6; MNI space coordinates = −2, 46, 20), dorsal ACC (peak Z score = 7.68; MNI space coordinates = −2, 36, 18; $p < .05$ FWE), right OFC (peak Z score = 10.3; MNI space coordinates = 52, 22, −10; $p < .05$ FWE), and right hippocampus/amygdala complex (peak Z score = 8.82; MNI space coordinates = 28, −16, −22; $p < .05$ FWE). A complete list of all significant clusters is provided in Table 2. It is important to note again that activity in these brain areas covaried with congruent Pavlovian and instrumental predictions in both the aversive and appetitive domains.

Consistent with the task-informed analysis, we did not find any significant clusters to be negatively correlated with the model-informed interaction regressor. One possible explanation is that competition interaction effects are being absorbed by instrumental and Pavlovian main effects and the neural mechanisms of competition are being implemented in the premotor areas subserving instrumental control.

PII Synergistic Neural Effects Scale with Behavioral Performance in Cooperation Conditions

We reasoned that BOLD activity reflecting Pavlovian and instrumental synergistic effects should scale with observed task performance during congruent trials when both Pavlovian and instrumental predictions prescribe the same motor responses.

On the basis of the extensive literature on the key role of the amygdala in the context of PIT (Cartoni, Balleine, & Baldassarre, 2016), we first investigated this region and found that its hemodynamic activity was significantly correlated with performance in the congruent, $r_{\text{bend}}(38) = .38$, $p = .015$, but not in the incongruent, $r_{\text{bend}}(38) = -.05$, $p = .77$, trials (Figure 4G and E). As we compared correlation coefficients, we found a significant difference (r_{cong}–$r_{\text{incong}} = .41$ [.01–.77], $p = .041$), thus confirming a significant interaction and pointing to a specific effect of amygdalar activity on task performance in response to congruent cues. As we further dissected activity in this region by cue type, we found evidence of temporal disambiguation of the PII neural effects along the valence axis with an earlier peak for the aversive congruent cues and a later peak for the appetitive congruent cues (Figure 4C).

We also investigated BOLD responses in other brain regions pertaining to the limbic system (including the PCC, dorsal ACC, and right OFC) and medial pFC. In the PCC, we observed an analogous activity pattern to the right amygdala/hippocampus complex (Figure 4C). Similarly, individual task performance scaled with mean PCC hemodynamic responses to congruent, $r_{\text{bend}}(38) = .35$, $p = .025$, but not incongruent, $r_{\text{bend}}(38) = .04$, $p = .79$, cues (Figure 4E and G), although in this case, interaction was statistically nonsignificant ($r_{\text{cong}}-r_{\text{incong}} = .31$ [−.08–.67], $p = .12$). A less prominent two-peak activity pattern was still discernible in the dorsal ACC (Figure 7A), although it did not significantly correlate with behavior (congruent cues: $r_{\text{bend}}(38) = .087$, $p = .59$; incongruent cues: $r_{\text{bend}}(38) = .11$, $p = .51$). We found positive BOLD responses in the medial pFC (Figure 7C) and in the right OFC (Figure 7E) to be valence dependent as they were predominantly elicited by appetitive and aversive congruent cues, respectively. However, we did not detect any significant BOLD–behavior correlations in the medial pFC (congruent cues: $r_{\text{bend}}(38) = .23$, $p = .16$; incongruent cues: $r_{\text{bend}}(38) = .18$, $p = .26$) nor the right OFC (congruent cues: $r_{\text{bend}}(38) = .17$, $p = .29$; incongruent cues: $r_{\text{bend}}(38) = -.12$, $p = .44$).

DISCUSSION

Dissecting the functional neuroanatomy of associative learning can afford invaluable insights into the neural mechanisms underlying adaptive and maladaptive decision-making. Accordingly, the neural underpinnings of the two-process learning theory have been extensively researched predominantly in animals but more recently in humans. Computational methods have made a meaningful contribution to advancing our mechanistic understanding of how Pavlovian and instrumental valuation systems shape learning and oversee action control (Dorfman & Gershman, 2019; Guitart-Masip, Huys et al., 2012). Furthermore, combining computational approaches with neuroimaging techniques has yielded a powerful analysis tool to probe the neural pathways mediating associative learning and conditioned behavior (O'Doherty, Hampton, & Kim, 2007). Nonetheless, the experimental paradigms so far employed in this line of research such as the PIT and orthogonalized go/no-go tasks have failed to completely unlock the explanatory potential of modeling work. In this study, we devised a variation of the popular orthogonalized go/no-go task that permitted updating Pavlovian value in the absence of any instrumental learning. This simple refinement of the task design enabled us to better decorrelate the temporal evolution of Pavlovian and instrumental predictions associated with a given cue and model trial-by-trial updating of Pavlovian and instrumental contingencies. Moreover, we were able to describe neural interaction effects dynamically rather than in the absence of any new learning as it is the case in the conventional PIT paradigms. Using a model-informed imaging analysis approach, we identified distinct fMRI activation clusters encoding instrumental and Pavlovian predictions of future payoff in the SMC and vmPFC, respectively. Crucially, activity in the SMC could not be simply accounted for by impending motor responses and replicated a prior finding from our laboratory that value-based decisions requiring an overt response are encoded in the SMC (Pisauro, Fouragnan, Retzler, & Philiastides, 2017). In humans, a previous functional neuroimaging study also found evidence for action value signals in the SMC

Downloaded from http://direct.mit.edu/jocn/article-pdf/35/12/2089/2170792/jocn_a_02062.pdf by University of Glasgow user on 05 June 2026

(Wunderlich et al., 2009). The action specificity of our instrumental regressor accounted for the observed activity in premotor areas, which are involved in representing and planning movement. It has been suggested that action values are encoded in the action space and embedded in premotor processing of action selection (Wunderlich, Rangel, & O'Doherty, 2010). Importantly, we have shown that modulation of mean SMC hemodynamic responses to incongruent cues was linked to successful instrumental responding. Furthermore, trial-by-trial oscillations in this activity were predictive of RT and accuracy, therefore casting this region as a focal neural hub of instrumental control.

Anatomically, the SMC is thought to be part of a frontal–subcortical network (Nachev et al., 2008; Aron et al., 2007), which is involved in cognitive processes such as conflict monitoring, detection, and resolution (usually referred to as cognitive control; Aron et al., 2007). The SMC has a "hyperdirect" connection to the subthalamic nucleus (Aron et al., 2007; Tanji, Kurata, & Okano, 1985), which it recruits to inhibit or slow down prepotent motor responses (Frank, Samanta, Moustafa, & Sherman, 2007; Aron & Poldrack, 2006) via suppression of thalamocortical activity (Mink, 1996). In addition to withholding prepotent motor responses, another important function of the SMC is altering movement plans and switching between actions or rules (Crone, Wendelken, Donohue, & Bunge, 2006; Rushworth, Hadland, Paus, & Sipila, 2002). The SMC thus seems ideally suited to enabling optimal action control in high-conflict situations. Unlike in a previous fMRI study where "learners" showed greater recruitment of bilateral IFG in response to no-go cues (Guitart-Masip, Huys et al., 2012), we did not find any evidence linking IFG to improved performance.

Altogether, our data seem to suggest that Pavlovian response biases are overcome through increased goal-directed cognitive control rather than attenuated Pavlovian value signals. We did in fact not find evidence that reduced neural encoding of Pavlovian value was correlated with improved performance as a function of congruence. Relatedly, previous research work employing EEG demonstrated that frontal midline theta activity suppressed Pavlovian response biases and improved choice accuracy (Csifcsak, Melsaeter, & Mittner, 2020; Swart et al., 2018; Cavanagh et al., 2013). Theta oscillations have been linked to the detection of response conflict (van Driel, Swart, Egner, Ridderinkhof, & Cohen, 2015; Cohen & Cavanagh, 2011), and their source has been traced back to the SMC (Cohen & Ridderinkhof, 2013). Furthermore, stronger EEG midfrontal–motor connectivity has been shown to be associated with the reduction of Pavlovian interference, suggesting that the SMC may modulate motor response threshold in conflict conditions (Swart et al., 2018; Philiastides, Biele, Vavatzanidis, Kazzer, & Heekeren, 2010).

The function of the vmPFC in human value-based decision-making has so far been characterized as heterogeneous. Indeed, the vmPFC has been extensively implicated in signaling value (Fouragnan, Retzler, Mullinger, & Philiastides, 2015; Bartra, McGuire, & Kable, 2013; Philiastides, Biele, & Heekeren, 2010) and, more specifically, has been found to be involved in the representation of action-specific value (FitzGerald, Friston, & Dolan, 2012), chosen stimulus value (independent of stimulus–action pairing; Wunderlich et al., 2010), probability of chosen action (Daw, O'Doherty, Dayan, Seymour, & Dolan, 2006), the prior belief that a choice is correct (Hampton, Bossaerts, & O'Doherty, 2006), reward expectations (Blair et al., 2006), expected reward value (H. Kim, Shimojo, & O'Doherty, 2006), and chosen (rostral) and unchosen (caudal) action expected value (Morris, Dezfouli, Griffiths, & Balleine, 2014). To the best of our knowledge, although there are no previous imaging studies that have documented Pavlovian value signals in the vmPFC or dorsal ACC, recent research work has reported positive and negative valence effects in these regions, consistent with our findings (Algermissen et al., 2022). In addition, outcome-locked vmPFC activity has been shown to scale with greater Pavlovian influence as a function of diminished environmental controllability (Gershman, Guitart-Masip, & Cavanagh, 2021). Notably, previous human imaging studies employed instrumental learning paradigms whereby Pavlovian predictions would have been updated based on instrumental performance and therefore resulting in instrumental predictions capturing neural activity linked to Pavlovian valuation. Although, in our task, we were not able to completely decorrelate Pavlovian and instrumental predictions because of the presence of mixed trials, we still found a noticeable valence effect (only marginally modulated by instrumental performance) in the vmPFC and dorsal ACC. The critical role of these regions in exerting motivational biases on behavior was corroborated by the findings that both vmPFC and dorsal ACC peak activity predicted trial-by-trial speeding up and slowing down of button presses. Furthermore, the observation that vmPFC activity did not correlate with performance as a function of congruence nor did it predict trial-wise choice accuracy suggested that the vmPFC is not directly involved in guiding action selection and resolving conflict.

Using classical or operant conditioning paradigms, human fMRI studies detected action (FitzGerald et al., 2012) and Pavlovian (Gottfried, O'Doherty, & Dolan, 2002; O'Doherty, Deichmann, Critchley, & Dolan, 2002) expected value signals in the striatum. Furthermore, previous work using the conventional version of the orthogonalized go/no-go task reported striatal hemodynamic activity during cue presentation predominantly represented action rather than valence effects (Guitart-Masip, Huys et al., 2012; Guitart-Masip, Fuentemilla et al., 2011). It is worth noting that, in Guitart-Masip, Fuentemilla, et al. (2011), participants were fully aware of cue–action couplings, which may have lessened motivational biases on action control. Nonetheless, the modulatory effect of valence on action representations in the striatum was still evident, albeit statistically nonsignificant (Guitart-Masip, Fuentemilla et al., 2011). In line with a

Downloaded from http://direct.mit.edu/jocn/article-pdf/35/12/2089/2170792/jocn_a_02062.pdf by University of Glasgow user on 05 June 2026

previous report (Algermissen et al., 2022), we found that BOLD activity in a cluster in the left medial caudate was significantly correlated with negative valence (whole-brain analysis) and negative Pavlovian value (ROI analysis). Remarkably, we did not detect any striatal activity covarying with trial-by-trial instrumental predictions nor positive Pavlovian value or PII effects. It is possible that the presence of Pavlovian-only trials in our task may have enhanced valence signals and diluted action representations in the striatum.

There exists a rich animal literature implicating the amygdala in different forms of PIT including conditioned suppression (i.e., an aversive Pavlovian conditioned stimulus decreases vigor of appetitive instrumental approach responding) and conditioned facilitation (i.e., an aversive Pavlovian conditioned stimulus increases vigor of aversive instrumental avoidance responding; Kim et al., 2022; Campese et al., 2017; Campese, Gonzaga, Moscarello, & LeDoux, 2015). Using congruent appetitive PIT paradigms, previous neuroimaging studies have found that BOLD activity in the nucleus accumbens (Mendelsohn, Pine, & Schiller, 2014; Talmi, Seymour, Dayan, & Dolan, 2008), amygdala (Mendelsohn et al., 2014; Prevost, Liljeholm, Tyszka, & O'Doherty, 2012; Talmi et al., 2008), and striatum (Prevost et al., 2012; Bray, Rangel, Shimojo, Balleine, & O'Doherty, 2008) is correlated with appetitive PIT effects. Furthermore, the amygdala and the nucleus accumbens have also been linked to aversive PIT and were activated in the context of behavioral inhibition elicited by aversive Pavlovian cues (Geurts et al., 2013). Our finding that the hippocampus/amygdala complex encodes congruent PII effects both in the aversive and appetitive domains thus reconciles previous neuroimaging reports and is supported by the observation of a significant correlation with performance during congruent trials. Intriguingly, the temporal dynamics of this effect are characterized by an earlier peak for aversive cues and a later peak for appetitive cues. Notably, a similar activity pattern was also observed in the PCC. Converging empirical evidence has established that the amygdala acquires information about the overall motivational value and salience of environmental stimuli and regulates motivated behavior (Morrison & Salzman, 2010). The amygdala does in fact encode information about both positively and negatively valenced stimuli (Ball et al., 2009), which it appraises in a context-dependent fashion, subsequently giving rises to decision biases (De Martino et al., 2006).

Our task did not permit identification of biases in instrumental learning. Swart et al. reported asymmetries in instrumental learning alongside already known Pavlovian-mediated response biases and showed that, compared to no-go responses, go responses were easier to learn and unlearn in the face of reward and punishment, respectively (Swart et al., 2017). Moreover, our task did not account for action specificity of Pavlovian influence on instrumental control across withdrawal and approach contexts (Huys et al., 2011). Finally, to conclusively rule out the biasing effect of motor confounds when assessing correlations between brain activity and performance, our task could be modified to ensure a comparable number of correct (or incorrect) trials across participants. Future imaging work leveraging the greater spatial resolution of ultra-high field fMRI may shed light on the human neural correlates of general and specific PIT effects, which have been well characterized in animals using lesion manipulations (Corbit & Balleine, 2011).

In conclusion, in this study, we have devised a novel version of a popular orthogonalized go/no-go task to better disentangle Pavlovian and instrumental neural representations and have expanded existing knowledge on the functional neuroanatomy of Pavlovian and instrumental processes underlying decision-making. We have shown that whereas the SMC encodes instrumental value and facilitates optimal instrumental responses detecting and overriding Pavlovian conflict, the vmPFC underpins Pavlovian valuation and gives rise to motivational biasing of behavior. Moreover, we have elucidated the role of the amygdala/hippocampus (and PCC) in implementing PII synergistic neural effects at different timescales across the negative and positive valence domains.

Acknowledgments

This work was supported by a Medical Research Council- and Medical Research Foundation-funded clinical research training fellowship (Psystar) awarded to F. Q.

Reprint requests should be sent to Filippo Queirazza, University of Glasgow, Glasgow, G12 0XH, United Kingdom, or via e-mail: Filippo.Queirazza@glasgow.ac.uk.

Data Availability Statement

Data and code will be made available upon reasonable request.

Author Contributions

Filippo Queirazza: Conceptualization; Data curation; Funding acquisition; Formal analysis; Investigation; Methodology; Project administration; Software; Visualization; Writing—Original draft; Writing—Review & editing. Rajeev Krishnadas: Writing—Review & editing. J. Douglas Steele: Writing—Review & editing. Jonathan Cavanagh: Writing—Review & editing. Marios G. Philiastides: Conceptualization; Formal analysis; Methodology; Software; Visualization; Writing—Review & editing.

Funding Information

Medical Research Foundation (https://dx.doi.org/10.13039/501100009187), grant number: Clinical Research Training Fellowship.

Diversity in Citation Practices

A retrospective analysis of the citations in every article published in this journal from 2010 to 2020 has revealed

Downloaded from http://direct.mit.edu/jocn/article-pdf/35/12/2089/2170792/jocn_a_02062.pdf by University of Glasgow user on 05 June 2026

a persistent pattern of gender imbalance: Although the proportions of authorship teams (categorized by estimated gender identification of first author/last author) publishing in the *Journal of Cognitive Neuroscience (JoCN)* during this period were M(an)/M = .408, W(oman)/M = .335, M/W = .108, and W/W = .149, the comparable proportions for the articles that these authorship teams cited were M/M = .579, W/M = .243, M/W = .102, and W/W = .076 (Fulvio et al., *JoCN*, 33:1, pp. 3–7). Consequently, *JoCN* encourages all authors to consider gender balance explicitly when selecting which articles to cite and gives them the opportunity to report their article's gender citation balance.

REFERENCES

Algermissen, J., Swart, J. C., Scheeringa, R., Cools, R., & den Ouden, H. E. M. (2022). Striatal BOLD and midfrontal theta power express motivation for action. *Cerebral Cortex*, *32*, 2924–2942. https://doi.org/10.1093/cercor/bhab391, PubMed: 34849626

Aron, A. R., Behrens, T. E., Smith, S., Frank, M. J., & Poldrack, R. A. (2007). Triangulating a cognitive control network using diffusion-weighted magnetic resonance imaging (MRI) and functional MRI. *Journal of Neuroscience*, *27*, 3743–3752. https://doi.org/10.1523/JNEUROSCI.0519-07.2007, PubMed: 17409238

Aron, A. R., & Poldrack, R. A. (2006). Cortical and subcortical contributions to stop signal response inhibition: Role of the subthalamic nucleus. *Journal of Neuroscience*, *26*, 2424–2433. https://doi.org/10.1523/JNEUROSCI.4682-05.2006, PubMed: 16510720

Ball, T., Derix, J., Wentlandt, J., Wieckhorst, B., Speck, O., Schulze-Bonhage, A., et al. (2009). Anatomical specificity of functional amygdala imaging of responses to stimuli with positive and negative emotional valence. *Journal of Neuroscience Methods*, *180*, 57–70. https://doi.org/10.1016/j.jneumeth.2009.02.022, PubMed: 19427530

Barr, D. J., Levy, R., Scheepers, C., & Tily, H. J. (2013). Random effects structure for confirmatory hypothesis testing: Keep it maximal. *Journal of Memory and Language*, *68*, 255–278. https://doi.org/10.1016/j.jml.2012.11.001, PubMed: 24403724

Bartra, O., McGuire, J. T., & Kable, J. W. (2013). The valuation system: A coordinate-based meta-analysis of BOLD fMRI experiments examining neural correlates of subjective value. *Neuroimage*, *76*, 412–427. https://doi.org/10.1016/j.neuroimage.2013.02.063, PubMed: 23507394

Beck, A., Schlagenhauf, F., Wustenberg, T., Hein, J., Kienast, T., Kahnt, T., et al. (2009). Ventral striatal activation during reward anticipation correlates with impulsivity in alcoholics. *Biological Psychiatry*, *66*, 734–742. https://doi.org/10.1016/j.biopsych.2009.04.035, PubMed: 19560123

Beckmann, C. F., Jenkinson, M., & Smith, S. M. (2003). General multilevel linear modeling for group analysis in FMRI. *Neuroimage*, *20*, 1052–1063. https://doi.org/10.1016/S1053-8119(03)00435-X, PubMed: 14568475

Blair, K., Marsh, A. A., Morton, J., Vythilingam, M., Jones, M., Mondillo, K., et al. (2006). Choosing the lesser of two evils, the better of two goods: Specifying the roles of ventromedial prefrontal cortex and dorsal anterior cingulate in object choice. *Journal of Neuroscience*, *26*, 11379–11386. https://doi.org/10.1523/JNEUROSCI.1640-06.2006, PubMed: 17079666

Bray, S., Rangel, A., Shimojo, S., Balleine, B., & O'Doherty, J. P. (2008). The neural mechanisms underlying the influence of pavlovian cues on human decision making. *Journal of Neuroscience*, *28*, 5861–5866. https://doi.org/10.1523/JNEUROSCI.0897-08.2008, PubMed: 18509047

Bretzke, M., Vetter, N. C., Kohls, G., Wahl, H., Roessner, V., Plichta, M. M., et al. (2023). Is loss avoidance differentially rewarding in adolescents versus adults? Differences in ventral striatum and anterior insula activation during the anticipation of potential monetary losses. *Cognitive Neuroscience*, *14*, 36–49. https://doi.org/10.1080/17588928.2022.2038555, PubMed: 35188088

Brown, P. L., & Jenkins, H. M. (1968). Auto-shaping of the pigeon's key-peck. *Journal of the Experimental Analysis of Behavior*, *11*, 1–8. https://doi.org/10.1901/jeab.1968.11-1, PubMed: 5636851

Campese, V. D., Gonzaga, R., Moscarello, J. M., & LeDoux, J. E. (2015). Modulation of instrumental responding by a conditioned threat stimulus requires lateral and central amygdala. *Frontiers in Behavioral Neuroscience*, *9*, 293. https://doi.org/10.3389/fnbeh.2015.00293, PubMed: 26578921

Campese, V. D., Soroeta, J. M., Vazey, E. M., Aston-Jones, G., LeDoux, J. E., & Sears, R. M. (2017). Noradrenergic regulation of central amygdala in aversive Pavlovian-to-instrumental transfer. *eNeuro*, *4* ENEURO.0224-17.2017. https://doi.org/10.1523/ENEURO.0224-17.2017, PubMed: 29071299

Cartoni, E., Balleine, B., & Baldassarre, G. (2016). Appetitive Pavlovian–instrumental transfer: A review. *Neuroscience & Biobehavioral Reviews*, *71*, 829–848. https://doi.org/10.1016/j.neubiorev.2016.09.020, PubMed: 27693227

Cartoni, E., Puglisi-Allegra, S., & Baldassarre, G. (2013). The three principles of action: A Pavlovian–instrumental transfer hypothesis. *Frontiers in Behavioral Neuroscience*, *7*, 153. https://doi.org/10.3389/fnbeh.2013.00153, PubMed: 24312025

Cavanagh, J. F., Eisenberg, I., Guitart-Masip, M., Huys, Q., & Frank, M. J. (2013). Frontal theta overrides pavlovian learning biases. *Journal of Neuroscience*, *33*, 8541–8548. https://doi.org/10.1523/JNEUROSCI.5754-12.2013, PubMed: 23658191

Chambers, C. D., Bellgrove, M. A., Stokes, M. G., Henderson, T. R., Garavan, H., Robertson, I. H., et al. (2006). Executive "brake failure" following deactivation of human frontal lobe. *Journal of Cognitive Neuroscience*, *18*, 444–455. https://doi.org/10.1162/089892906775990606, PubMed: 16513008

Cohen, M. X., & Cavanagh, J. F. (2011). Single-trial regression elucidates the role of prefrontal theta oscillations in response conflict. *Frontiers in Psychology*, *2*, 30. https://doi.org/10.3389/fpsyg.2011.00030, PubMed: 21713190

Cohen, M. X., & Ridderinkhof, K. R. (2013). EEG source reconstruction reveals frontal–parietal dynamics of spatial conflict processing. *PLoS One*, *8*, e57293. https://doi.org/10.1371/journal.pone.0057293, PubMed: 23451201

Corbit, L. H., & Balleine, B. W. (2011). The general and outcome-specific forms of Pavlovian–instrumental transfer are differentially mediated by the nucleus accumbens core and shell. *Journal of Neuroscience*, *31*, 11786–11794. https://doi.org/10.1523/JNEUROSCI.2711-11.2011, PubMed: 21849539

Crockett, M. J., Clark, L., & Robbins, T. W. (2009). Reconciling the role of serotonin in behavioral inhibition and aversion: Acute tryptophan depletion abolishes punishment-induced inhibition in humans. *Journal of Neuroscience*, *29*, 11993–11999. https://doi.org/10.1523/JNEUROSCI.2513-09.2009, PubMed: 19776285

Crone, E. A., Wendelken, C., Donohue, S. E., & Bunge, S. A. (2006). Neural evidence for dissociable components of

Downloaded from http://direct.mit.edu/jocn/article-pdf/35/12/2089/2170792/jocn_a_02062.pdf by University of Glasgow user on 05 June 2026

task-switching. *Cerebral Cortex*, *16*, 475–486. https://doi.org/10.1093/cercor/bhi127, PubMed: 16000652

Csifcsak, G., Melsaeter, E., & Mittner, M. (2020). Intermittent absence of control during reinforcement learning interferes with Pavlovian bias in action selection. *Journal of Cognitive Neuroscience*, *32*, 646–663. https://doi.org/10.1162/jocn_a_01515, PubMed: 31851595

Daw, N. D., O'Doherty, J. P., Dayan, P., Seymour, B., & Dolan, R. J. (2006). Cortical substrates for exploratory decisions in humans. *Nature*, *441*, 876–879. https://doi.org/10.1038/nature04766, PubMed: 16778890

Dayan, P., & Huys, Q. J. M. (2008). Serotonin, inhibition, and negative mood. *PLoS Computational Biology*, *4*, e4. https://doi.org/10.1371/journal.pcbi.0040004, PubMed: 18248087

De Martino, B., Kumaran, D., Seymour, B., & Dolan, R. J. (2006). Frames, biases, and rational decision-making in the human brain. *Science*, *313*, 684–687. https://doi.org/10.1126/science.1128356, PubMed: 16888142

Dorfman, H. M., & Gershman, S. J. (2019). Controllability governs the balance between Pavlovian and instrumental action selection. *Nature Communications*, *10*, 5826. https://doi.org/10.1038/s41467-019-13737-7, PubMed: 31862876

FitzGerald, T. H. B., Friston, K. J., & Dolan, R. J. (2012). Action-specific value signals in reward-related regions of the human brain. *Journal of Neuroscience*, *32*, 16417–16423a. https://doi.org/10.1523/JNEUROSCI.3254-12.2012, PubMed: 23152624

Fouragnan, E., Retzler, C., Mullinger, K., & Philiastides, M. G. (2015). Two spatiotemporally distinct value systems shape reward-based learning in the human brain. *Nature Communications*, *6*, 8107. https://doi.org/10.1038/ncomms9107, PubMed: 26348160

Frank, M. J., Samanta, J., Moustafa, A. A., & Sherman, S. J. (2007). Hold your horses: Impulsivity, deep brain stimulation, and medication in parkinsonism. *Science*, *318*, 1309–1312. https://doi.org/10.1126/science.1146157, PubMed: 17962524

Garbusow, M., Ebrahimi, C., Riemerschmid, C., Daldrup, L., Rothkirch, M., Chen, K., et al. (2022). Pavlovian-to-instrumental transfer across mental disorders: A review. *Neuropsychobiology*, *81*, 418–437. https://doi.org/10.1159/000525579, PubMed: 35843212

Gershman, S. J., Guitart-Masip, M., & Cavanagh, J. F. (2021). Neural signatures of arbitration between Pavlovian and instrumental action selection. *PLoS Computational Biology*, *17*, e1008553. https://doi.org/10.1371/journal.pcbi.1008553, PubMed: 33566831

Geurts, D. E. M., Huys, Q. J. M., den Ouden, H. E. M., & Cools, R. (2013). Aversive Pavlovian control of instrumental behavior in humans. *Journal of Cognitive Neuroscience*, *25*, 1428–1441. https://doi.org/10.1162/jocn_a_00425, PubMed: 23691985

Gottfried, J. A., O'Doherty, J., & Dolan, R. J. (2002). Appetitive and aversive olfactory learning in humans studied using event-related functional magnetic resonance imaging. *Journal of Neuroscience*, *22*, 10829–10837. https://doi.org/10.1523/JNEUROSCI.22-24-10829.2002, PubMed: 12486176

Greve, D. N., & Fischl, B. (2009). Accurate and robust brain image alignment using boundary-based registration. *Neuroimage*, *48*, 63–72. https://doi.org/10.1016/j.neuroimage.2009.06.060, PubMed: 19573611

Guitart-Masip, M., Chowdhury, R., Sharot, T., Dayan, P., Duzel, E., & Dolan, R. J. (2012). Action controls dopaminergic enhancement of reward representations. *Proceedings of the National Academy of Sciences, U.S.A.*, *109*, 7511–7516. https://doi.org/10.1073/pnas.1202229109, PubMed: 22529363

Guitart-Masip, M., Fuentemilla, L., Bach, D. R., Huys, Q. J. M., Dayan, P., Dolan, R. J., et al. (2011). Action dominates valence in anticipatory representations in the human striatum and dopaminergic midbrain. *Journal of Neuroscience*, *31*, 7867–7875. https://doi.org/10.1523/JNEUROSCI.6376-10.2011, PubMed: 21613500

Guitart-Masip, M., Huys, Q. J. M., Fuentemilla, L., Dayan, P., Duzel, E., & Dolan, R. J. (2012). Go and no-go learning in reward and punishment: Interactions between affect and effect. *Neuroimage*, *62*, 154–166. https://doi.org/10.1016/j.neuroimage.2012.04.024, PubMed: 22548809

Hampton, A. N., Bossaerts, P., & O'Doherty, J. P. (2006). The role of the ventromedial prefrontal cortex in abstract state-based inference during decision making in humans. *Journal of Neuroscience*, *26*, 8360–8367. https://doi.org/10.1523/JNEUROSCI.1010-06.2006, PubMed: 16899731

Huys, Q. J. M., Cools, R., Gölzer, M., Friedel, E., Heinz, A., Dolan, R. J., et al. (2011). Disentangling the roles of approach, activation and valence in instrumental and Pavlovian responding. *PLoS Computational Biology*, *7*, e1002028. https://doi.org/10.1371/journal.pcbi.1002028, PubMed: 21556131

Huys, Q. J. M., Gölzer, M., Friedel, E., Heinz, A., Cools, R., Dayan, P., et al. (2016). The specificity of Pavlovian regulation is associated with recovery from depression. *Psychological Medicine*, *46*, 1027–1035. https://doi.org/10.1017/S0033291715002597, PubMed: 26841896

Jenkinson, M. (2003). Fast, automated, *N*-dimensional phase-unwrapping algorithm. *Magnetic Resonance in Medicine*, *49*, 193–197. https://doi.org/10.1002/mrm.10354, PubMed: 12509838

Jenkinson, M., Bannister, P., Brady, M., & Smith, S. (2002). Improved optimization for the robust and accurate linear registration and motion correction of brain images. *Neuroimage*, *17*, 825–841. https://doi.org/10.1006/nimg.2002.1132, PubMed: 12377157

Jenkinson, M., & Smith, S. (2001). A global optimisation method for robust affine registration of brain images. *Medical Image Analysis*, *5*, 143–156. https://doi.org/10.1016/S1361-8415(01)00036-6, PubMed: 11516708

Kahneman, D., Knetsch, J. L., & Thaler, R. H. (1990). Experimental tests of the endowment effect and the Coase theorem. *Journal of Political Economy*, *98*, 1325–1348. https://doi.org/10.1086/261737

Kim, I. T., Farb, C., Hou, M., Prasad, S., Talley, E., Cook, S., et al. (2022). General and specific aversive modulation of active avoidance require central amygdala. *Frontiers in Behavioral Neuroscience*, *16*, 879168. https://doi.org/10.3389/fnbeh.2022.879168, PubMed: 35795380

Kim, H., Shimojo, S., & O'Doherty, J. P. (2006). Is avoiding an aversive outcome rewarding? Neural substrates of avoidance learning in the human brain. *PLoS Biology*, *4*, e233. https://doi.org/10.1371/journal.pbio.0040233, PubMed: 16802856

Mackintosh, N. J. (1983). *Conditioning and associative learning*. Oxford, UK: Clarendon Press.

Mendelsohn, A., Pine, A., & Schiller, D. (2014). Between thoughts and actions: Motivationally salient cues invigorate mental action in the human brain. *Neuron*, *81*, 207–217. https://doi.org/10.1016/j.neuron.2013.10.019, PubMed: 24333054

Mink, J. W. (1996). The basal ganglia: Focused selection and inhibition of competing motor programs. *Progress in Neurobiology*, *50*, 381–425. https://doi.org/10.1016/S0301-0082(96)00042-1, PubMed: 9004351

Mkrtchian, A., Aylward, J., Dayan, P., Roiser, J. P., & Robinson, O. J. (2017). Modeling avoidance in mood and anxiety disorders using reinforcement learning. *Biological Psychiatry*, *82*, 532–539. https://doi.org/10.1016/j.biopsych.2017.01.017, PubMed: 28343697

Morris, R. W., Dezfouli, A., Griffiths, K. R., & Balleine, B. W. (2014). Action–value comparisons in the dorsolateral

Downloaded from http://direct.mit.edu/jocn/article-pdf/35/12/2089/2170792/jocn_a_02062.pdf by University of Glasgow user on 05 June 2026

prefrontal cortex control choice between goal-directed actions. *Nature Communications*, *5*, 4390. https://doi.org/10.1038/ncomms5390, PubMed: 25055179

Morrison, S. E., & Salzman, C. D. (2010). Re-valuing the amygdala. *Current Opinion in Neurobiology*, *20*, 221–230. https://doi.org/10.1016/j.conb.2010.02.007, PubMed: 20299204

Nachev, P., Kennard, C., & Husain, M. (2008). Functional role of the supplementary and pre-supplementary motor areas. *Nature Reviews Neuroscience*, *9*, 856–869. https://doi.org/10.1038/nrn2478, PubMed: 18843271

Nachev, P., Rees, G., Parton, A., Kennard, C., & Husain, M. (2005). Volition and conflict in human medial frontal cortex. *Current Biology*, *15*, 122–128. https://doi.org/10.1016/j.cub.2005.01.006, PubMed: 15668167

Nieuwenhuis, S., Forstmann, B. U., & Wagenmakers, E. J. (2011). Erroneous analyses of interactions in neuroscience: A problem of significance. *Nature Neuroscience*, *14*, 1105–1107. https://doi.org/10.1038/nn.2886, PubMed: 21878926

O'Doherty, J. P., Deichmann, R., Critchley, H. D., & Dolan, R. J. (2002). Neural responses during anticipation of a primary taste reward. *Neuron*, *33*, 815–826. https://doi.org/10.1016/S0896-6273(02)00603-7, PubMed: 11879657

O'Doherty, J. P., Hampton, A., & Kim, H. (2007). Model-based fMRI and its application to reward learning and decision making. *Annals of the New York Academy of Sciences*, *1104*, 35–53. https://doi.org/10.1196/annals.1390.022, PubMed: 17416921

Ousdal, O. T., Huys, Q. J., Milde, A. M., Craven, A. R., Ersland, L., Endestad, T., et al. (2018). The impact of traumatic stress on Pavlovian biases. *Psychological Medicine*, *48*, 327–336. https://doi.org/10.1017/S003329171700174X

Palminteri, S., Wyart, V., & Koechlin, E. (2017). The importance of falsification in computational cognitive modeling. *Trends in Cognitive Sciences*, *21*, 425–433. https://doi.org/10.1016/j.tics.2017.03.011, PubMed: 28476348

Philiastides, M. G., Biele, G., & Heekeren, H. R. (2010). A mechanistic account of value computation in the human brain. *Proceedings of the National Academy of Sciences, U.S.A.*, *107*, 9430–9435. https://doi.org/10.1073/pnas.1001732107, PubMed: 20439711

Philiastides, M. G., Biele, G., Vavatzanidis, N., Kazzer, P., & Heekeren, H. R. (2010). Temporal dynamics of prediction error processing during reward-based decision making. *Neuroimage*, *53*, 221–232. https://doi.org/10.1016/j.neuroimage.2010.05.052, PubMed: 20510376

Pisauro, M. A., Fouragnan, E., Retzler, C., & Philiastides, M. G. (2017). Neural correlates of evidence accumulation during value-based decisions revealed via simultaneous EEG–fMRI. *Nature Communications*, *8*, 15808. https://doi.org/10.1038/ncomms15808, PubMed: 28598432

Prevost, C., Liljeholm, M., Tyszka, J. M., & O'Doherty, J. P. (2012). Neural correlates of specific and general Pavlovian-to-instrumental transfer within human amygdalar subregions: A high-resolution fMRI study. *Journal of Neuroscience*, *32*, 8383–8390. https://doi.org/10.1523/JNEUROSCI.6237-11.2012, PubMed: 22699918

Rescorla, R. A., & Solomon, R. L. (1967). Two-process learning theory: Relationships between Pavlovian conditioning and instrumental learning. *Psychological Review*, *74*, 151–182. https://doi.org/10.1037/h0024475, PubMed: 5342881

Robinson, T. E., & Berridge, K. C. (2003). Addiction. *Annual Review of Psychology*, *54*, 25–53. https://doi.org/10.1146/annurev.psych.54.101601.145237, PubMed: 12185211

Rushworth, M. F. S., Hadland, K. A., Paus, T., & Sipila, P. K. (2002). Role of the human medial frontal cortex in task switching: A combined fMRI and TMS study. *Journal of Neurophysiology*, *87*, 2577–2592. https://doi.org/10.1152/jn.2002.87.5.2577, PubMed: 11976394

Smith, S. M., Jenkinson, M., Woolrich, M. W., Beckmann, C. F., Behrens, T. E. J., Johansen-Berg, H., et al. (2004). Advances in functional and structural MR image analysis and implementation as FSL. *Neuroimage*, *23(Suppl. 1)*, S208–S219. https://doi.org/10.1016/j.neuroimage.2004.07.051, PubMed: 15501092

Swart, J. C., Frank, M. J., Maatta, J. I., Jensen, O., Cools, R., & den Ouden, H. E. M. (2018). Frontal network dynamics reflect neurocomputational mechanisms for reducing maladaptive biases in motivated action. *PLoS Biology*, *16*, e2005979. https://doi.org/10.1371/journal.pbio.2005979, PubMed: 30335745

Swart, J. C., Frobose, M. I., Cook, J. L., Geurts, D. E., Frank, M. J., Cools, R., et al. (2017). Catecholaminergic challenge uncovers distinct Pavlovian and instrumental mechanisms of motivated (in)action. *eLife*, *6*, e22169. https://doi.org/10.7554/eLife.22169, PubMed: 28504638

Talmi, D., Seymour, B., Dayan, P., & Dolan, R. J. (2008). Human Pavlovian–instrumental transfer. *Journal of Neuroscience*, *28*, 360–368. https://doi.org/10.1523/JNEUROSCI.4028-07.2008, PubMed: 18184778

Tanji, J., Kurata, K., & Okano, K. (1985). The effect of cooling of the supplementary motor cortex and adjacent cortical areas. *Experimental Brain Research*, *60*, 423–426. https://doi.org/10.1007/BF00235940, PubMed: 4054286

van Driel, J., Swart, J. C., Egner, T., Ridderinkhof, K. R., & Cohen, M. X. (2015). (No) time for control: Frontal theta dynamics reveal the cost of temporally guided conflict anticipation. *Cognitive, Affective & Behavioral Neuroscience*, *15*, 787–807. https://doi.org/10.3758/s13415-015-0367-2, PubMed: 26111755

Weiskopf, N., Hutton, C., Josephs, O., & Deichmann, R. (2006). Optimal EPI parameters for reduction of susceptibility-induced BOLD sensitivity losses: A whole-brain analysis at 3 T and 1.5 T. *Neuroimage*, *33*, 493–504. https://doi.org/10.1016/j.neuroimage.2006.07.029, PubMed: 16959495

Wilcox, R. R. (2016). Comparing dependent robust correlations. *British Journal of Mathematical and Statistical Psychology*, *69*, 215–224. https://doi.org/10.1111/bmsp.12069, PubMed: 27114391

Williams, D. R., & Williams, H. (1969). Auto-maintenance in the pigeon: Sustained pecking despite contingent non-reinforcement. *Journal of the Experimental Analysis of Behavior*, *12*, 511–520. https://doi.org/10.1901/jeab.1969.12-511, PubMed: 16811370

Wunderlich, K., Rangel, A., & O'Doherty, J. P. (2009). Neural computations underlying action-based decision making in the human brain. *Proceedings of the National Academy of Sciences, U.S.A.*, *106*, 17199–17204. https://doi.org/10.1073/pnas.0901077106, PubMed: 19805082

Wunderlich, K., Rangel, A., & O'Doherty, J. P. (2010). Economic choices can be made using only stimulus values. *Proceedings of the National Academy of Sciences, U.S.A.*, *107*, 15005–15010. https://doi.org/10.1073/pnas.1002258107, PubMed: 20696924

Downloaded from http://direct.mit.edu/jocn/article-pdf/35/12/2089/2170792/jocn_a_02062.pdf by University of Glasgow user on 05 June 2026